OPERATIONAL TRANSRESISTANCE AMPLIFIER AND ITS APPLICATIONS

A dissertation submitted in partial fulfillment of the requirement for the degree of

Master of Technology

In

VLSI Design and Embedded System

by

Shobha Mandal

(Roll No.- **2K17/VLS/18**)

Under the guidance of

Prof. Rajeshwari Pandey

DEPARTMENT OF ELECTRONICS AND COMMUNICATION ENGINEERING

DELHI TECHNOLOGICAL UNIVERSITY

DELHI – 110042

SEPTEMBER, 2019

CANDIDATE'S DECLARATION

I, **Shobha Mandal** (2K17/VLS/18) hereby declare that the project dissertation titled "**Operational Transresistance Amplifier and Its Application**" is submitted by me to the Department of Electronics and Communication, Delhi Technological University, New Delhi in partial fulfillment of the requirement for the award of the degree of Master of Technology is original and not copied from any source without proper citation. This work has not been previously formed the basis for the award of any degree, diploma, associateship, fellowship or other similar title or recognition to the best of my knowledge and belief.

Shobha Mandal

Place: New Delhi

Date: _____

CERTIFICATE

This is certified that the thesis work contained in this dissertation entitled "OPERATIONAL TRANSRESISTANCE AMPLIFIER AND ITS APPLICATIONS," by **Shobha mandal (2K17/VLS/18)** has been carried out under my supervision for award of the degree of **"MASTER OF TECHNOLOGY"** in **VLSI Design And Embedded System** of Delhi Technological University, New Delhi. This project was carried out under my supervision and has not been submitted anywhere else, either in part or full, for the award of any other degree or diploma to the best of my knowledge and belief.

Date _____

Prof. R. Pandey

SUPERVISOR

Professor, ECE Department

Delhi Technological University

ACKNOWLEDGEMENT

It gives me immense pleasure to express my deepest sense of gratitude and sincere thanks to my highly respected and esteemed guide **Prof. R. Pandey (Professor, ECE Department)** for her valuable guidance, encouragement and help for completing this work. Her useful suggestions for this whole work and co-operative behavior are sincerely acknowledged.

I would also like to express my sincere thanks to Mr. Gurumurthy, ex-phd scholar, DTU, my parents and some of my friends who helped me directly or indirectly to complete this thesis work.

Shobha Mandal

(2K17/VLS/18)

ABSTRACT

Sinusoidal oscillators are crucial part of any electrical and electronic applications like AC machine control systems, measurement meters, medical equipment, communication modules, control & instrumentation systems etc. A single OTRA based sinusoidal oscillator having independent control on condition of oscillation and frequency of oscillation is realized. A quadrature phase oscillator is also presented.

In any communication system oscillator is an inevitable block. Different modulation schemes namely DSB-SC, DSB-FC, PAM and one demodulation scheme (DSB-SC) have been realized using OTRA.

All the circuits are implemented using OTRA and their workability is verified through PSPICE using 180nm process parameters. The supply voltages used are ±1.5V. All simulation results are found to be in closed agreement with the theoretical results.

LIST OF FIGURES

LIST OF TABLES

LIST OF ABBREVIATIONS

AM: Amplitude Modulation

ASK: Amplitude Shift Keying

CMOS: Complementary MOS(MOSFET Oxide)

CO: Condition of Oscillation

DSB-SC: Double Side Band Suppressed Carrier

DSB-FC: Double Side Band Full Carrier

FO: Frequency of Oscillation

IC: Integrated Circuit

IF: Intermediate Frequency

HDTV: High Definition Televiosion

NTSC: National Television System Committee

PAM: Pulse Amplitude Modulation

PSK: Phase Shift Keying

OTRA: Operational Transresistance Amplifier

RF: Radio Frequency

TSMC: Taiwan Semiconductor Manufacturing Company

VLSI: Very Large Scale Integration

TABLE OF CONTENTS

Contents

INTRODUCTION

The world we live in is mostly analog in nature. However to make computing easier analog signals are converted into digital maintaining a degree of precision and then produced final output that is to be converted back into analog again. However in application areas such as sensor designing, mobile communication systems, memories and microprocessors, replacing analog functions with their digital counterparts is really hard, despite the advancement in CMOS technology. Current trend of designers is to design mixed-mode integrated circuits that can process both analog and digital signals on a single semiconductor die.

In the field of analog signal processing traditional voltage mode opamp has been the most versatile and common construction block. Opamp can amplify any input so effortlessly and can be used as a buffer. Along with some passive elements opamp can generate any simple to most complex functions. Generally negative feedback is used in opamp-circuits. Schmitt trigger and multivibrators are the some uses of positive feedbacked opamp. All these circuits are voltage mode(VM) circuits since both input and output are voltages. VM circuits yield many drawbacks like constant gain bandwidth product(GBP), gain bandwidth coupling, lower slew rate which affects the large signal and high frequency operation. Current mode(CM) circuits are superior in avoiding these drawbacks. In a CM structure information is conveyed using current signal rather than voltage signal. A brief comparison between current mode vs voltage mode circuits is discussed in the next section.

1.1 VOLTAGE MODE Vs. CURRENT MODECIRCUITS

Voltage mode signaling is most widely used in VLSI chips. In voltage mode signaling, receiver provides high input impedance(ideally infinity). The information is conveyed in the form of voltage and the output voltage is a function of input signal and is varied according to the supply voltage. Fig.1.1 shows the theoretical model of conventional voltage mode interconnection[1]. The output is terminated by an open circuit.

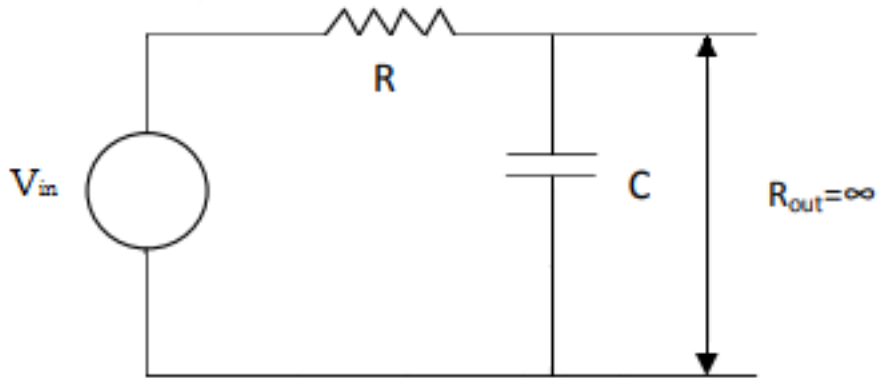

Fig 1.1 Voltage mode signaling

i. Since at the receiver end output impedance is so high, accumulated charges do not get effective discharging path to the ground. So voltage mode signaling circuits suffer from large delay.
ii. Stray or parasitic capacitances are found at high frequency and mid-frequency applications of VM circuits.
iii. The high-valued resistors with parasitic capacitances create a dominant pole at a relative low frequency that limits the bandwidth(BW).
iv. BW is also affected by unity gain BW property.
v. Even if there is a sudden change in the input voltage output voltage cannot change instantly.
vi. VM circuits need high supply voltages to get better SNR. Slew rate depends on the circuit time constants.

Due to all these reasons VM circuits are not suitable for high frequency applications and CM acts as a better alternative.

In current mode signaling, information is represented as current signal. The receiver provides very low impedance (ideally zero) at its input. In current mode signaling, line is terminated by shorting the wire. The theoretical model of current mode signaling[1] is as shown in Fig. 1.2.

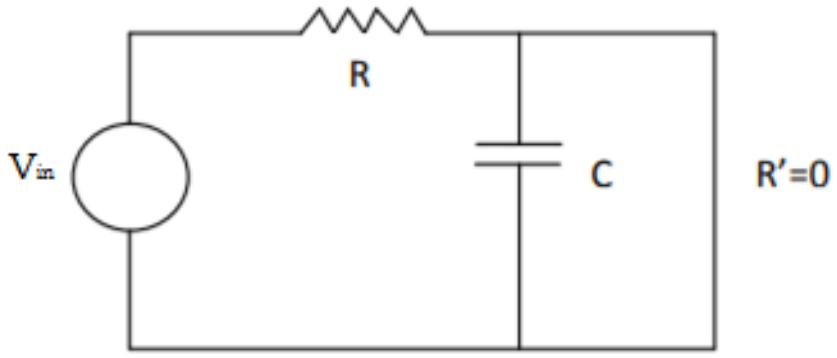

Fig. 1.2 Current mode signaling

Advantages of CM over VM are given below :

i. Bandwidth (BW) independent closed loop gain.
ii. Wide and nearly constant BW.
iii. Almost linear AC response.
iv. Operations like addition, subtraction, multiplication on signals become easier.
v. High dynamic range and relatively higher slew rate.
vi. High performance in terms of BW and speed.

However CM circuits also suffer from few problems like extra current sensing device at the output that increases power loss, area requirements and complexity. Current sensing must be very wideband to accurately reconstruct the current signal[2]. Another major problem in any CM circuit is lower SNR due to noise in the sensed current signal. At the cost of larger noise CM devices give higher speed and are therefore harder to maintain in stable condition or not to oscillate. Current amplifiers suffer from a larger input offset variations compared to high impedance voltage controlled devices.

In 1968, Sedra and Smith first introduced the concept of current conveyor which was the first current mode device.

During the last three to four decades a significant number of analog circuits have come out beyond the popular operational amplifier, operational transconductance amplifier, current conveyors etc. Among the incipient building blocks, the operational transresistance amplifier(OTRA) has received extensive interest and attention by the researchers. On the other hand there happened an evolution in the digital industry as well. And now in 21st century it is possible to integrate as high as hundred millions of transistors on a single chip or die using very large scale integration(VLSI) technology.

1.2 WHY OTRA

Generally operational transresistance amplifier is chosen over other conventional CM & VM circuits to avail the benefits of both current mode and voltage mode circuits in a single device. In an OTRA the input is current while the output is voltage. Due to which it becomes suitable in any hybrid circuit and we don't need transducer to change the form of the signal. Concept of virtual ground is applicable on OTRA that makes stray capacitances ineffective and makes suitable for high frequency applications. Output impedance of OTRA is very low making it adequate to cascade. Researchers have taken OTRA into account due to its inherent advantages like bandwidth independent closed loop gain, higher slew rate along with all the above mentioned properties.

1.3 OBJECTIVE

The first intention of this thesis is to characterize a CMOS OTRA with low supply voltage and low bias current. Then appications of this OTRA are developed. The objectives of this thesis are identified as:

i. Implementation of a CMOS OTRA
ii. Implementation of OTRA based oscillator
iii. Implementation of various modulation & demodulation schemes using OTRA.

1.4 ORGANIZATION OF THE THESIS

This dissertation is intended to study and analyse CMOS based Operational Transconductance Amplifier and its various communication applications as an oscillator. The project is done using PSPICE with parameter files by TSMC (350nm & 180nm).

Chapter 2: Literature review is presented.

Chapter 3: Characteristics of OTRA and its CMOS implementation have been discussed.

Chapter 4: Implementation of sinusoidal oscillator using OTRA is presented and compared with previous design. One quadrature oscillator has been designed with the help of this sinusoidal oscillator.

Chapter 5: The use of oscillator in communication system is very vast. With the sinusoidal oscillator different modulation and demodulation schemes have been implemented and verified.

Chapter 6: In this chapter the thesis work has been concluded with future scope of possibilities.

LITERATURE REVIEW

In the late 19th century when researchers got to know the benefits of hybrid-mode devices, invention of transconductance and transimpedance devices happened. In 1992 J. J. Chen et al. proposed an OTRA which was implemented using a differential current controlled current source which is followed by a voltage buffer[3]. In 1999 Salama et al. proposed a CMOS OTRA circuit[4] based on the feedback connection of modified differential current conveyor circuit(MDCC) and a common source amplifier[5].

The OTRA given in [6] comprised of low voltage regulated cascode current mirror with a low voltage regulated cascode load as the core of the circuit, common source amplifiers gain boosting stage and level shifters followed by common source output stage. In 2006 H. Mostafa et. al proposed a CMOS OTRA that used as low as fourteen transistors. It was based on the concept of current mirroring and was a modified version of Salama's OTRA reported in [4]. This decreases the impact of transistor error mismatch and increases operating range of frequency. Since it has smaller number of transistors, power consumption is reduced. A Rahman et. al modified Mostafa's OTRA with differential gain stages[7] rather common source stages to decrease the DC offset current and increases the DC open loop transresistance gain. Above reported all the OTRAs are CMOS based. However OTRA can be realized using two AD844N ICs[8] which is basically a current coveyor. A nullor based model is available in [9] where three grounded resistors and four nullors have been used to design a behavioral model at the circuit level of abstraction and is therefore extremely useful in CAD tools.

OpAmps have been used as the active element to make sinusoidal oscillators for decades but they lack excellent performance in high frequency applications(>100KHz). For the first time in 2000 oscillator using OTRA as active component has been reported[10] by Salama et. al. It was single phase sinusoidal oscillator with some passive elements. A single OTRA based oscillator is reported in [11]. These oscillators have

very complex CO and FO and they don't have independent control over CO and FO. Two novel oscillators reported in [12-13] solved the problem of interactive control of FO over CO. In [13] a general scheme to realize third order or multiphase($n \geq 3$) oscillator is shown. With the help of n-OTRAs it can produce n-odd and/or n-odd/even phased waveforms with automatic gain control(AGC). The purpose of AGC is to maintain a suitable signal amplitude at its output despite variation in the input. In [14], one Multiphase Sinusoidal Oscillator(MSO) is reported based on all pass network configuration. It requires n-OTRAs, (n+2)-resistors & n-capacitors to realize odd phased MSO and 2n-OTRAs, (n+5)-resistors & n-capacitors for even phased MSOs. Nagar e. al have presented two OTRA based third order quadrature oscillator[15] with only four resistors and three capacitors. FO and CO can be orthogonally controllable. A new quadrature oscillator reported in [16] has independent control over its CO & FO. It is based on the concept of forming closed loop using one high pass filter and one differentiator. MOS-C realization of oscillators[15-16] have been given for better integration.

There are various applications of OTRA from simple differentiator/integrator to circuits like multivibrators and filters. Voltage mode integrators using OTRA are reported in [4], [17-18]. All of these circuits are based on MOSFET-C, so reduced parasitic elements and higher density are the main advantages.

OTRA has been widely used to realise continuous time filters. OTRA based filters can be broadly classified into two types: first order continuous time active filters[19-21] and second or higher order continuous time active filters. Based on number of input and output terminals the latter can further be classified into four types: SISO(Single Intput Single Ouput)[22-29], SIMO(Single Input Multiple Output)[30-34], MISO(Multiple Intput Single Ouput)[35-36,43] type filters. Some of these filters are universal type[24,33,36] and can realize all the basic filtering functions like LP, HP, BP, BR & AP. Later in the thesis a MISO third order voltage mode filter reported in [43] is used later in this project for modulation and demodulation purposes.

Different methods of implementation of OTRA have been discussed in this literarature. And then existing OTRA based waveform generators are reviewed and a brief on existing OTRA based filters is presented.

CHAPTER 3

OTRA IMPLEMENTATION AND ANALYSIS

3.1 INTRODUCTION

An operational transresistance ampliflier (often OTRA)[4] is a high gain current input voltage output device. The phrase 'transresistance' is there because it converts input current into output voltage and the efficiency is measured in units of resistance. OTRA has very high input and output impedances that result in insensitivity to stray capacitances making it suitable for high frequency applications. The circuit symbol and the equivalent circuit of OTRA are shown in the below figures. The basic working principle[4] of OTRA is to sense the difference of input currents at the positive and negative input terminals ('p' & 'n') and then magnify the difference and produce voltage as output at the output terminal.

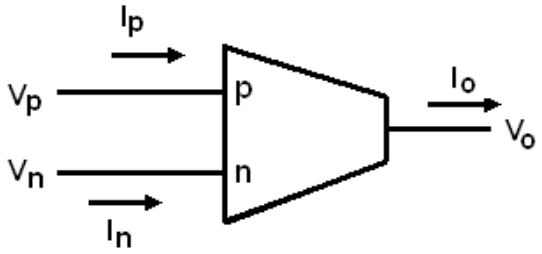

Fig 3.1 OTRA circuit Symbol[4]

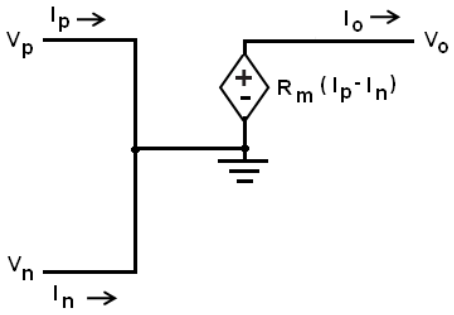

Fig 3.2 Equivalent circuit (ideal)[4]

Ideally an OTRA is supposed to act as an infinite gain amplifier and for this to happen voltages at input terminals should be zero and the gain of the amplifier should depend only

on the difference of the input currents not on individual values. The output voltage should also be independent of the current taken by the load impedance. Thus transresistance gain R_m approaches to infinity. Port characteristics of ideal OTRA is given by the below matix[5].

$$\begin{bmatrix} v_p \\ v_n \\ v_o \end{bmatrix} = \begin{bmatrix} 0 & 0 & 0 \\ 0 & 0 & 0 \\ R_m & -R_m & 0 \end{bmatrix} \begin{bmatrix} I_p \\ I_n \\ I_o \end{bmatrix} \quad (3.1)$$

From the above matrix v_o can be computed as,

$$v_o = I_p R_m - I_n R_m \quad (3.2)$$

In equation (3.2) we can see that the output voltage v_o can be represented as the difference of input current, multiplied with the tranresistance gain R_m.

Ideally $I_p = I_n$

And $R_m = \infty$

3.1.1 NON-IDEAL MODEL OF OTRA

While the above mentioned idealized conditions cannot be met in practice, the employment of ideal OTRA model simplifies the mathematical analysis of OTRA circuits. Practical OTRA circuits are made to approximate the idealized characteristics. In practice tranresistance gain R_m is high and in the range of MΩ or more than that. Practical equivalent circuit of OTRA is shown in the Fig 3.3 where R_p and R_n represent both the 'p' and 'n' terminal resistances respectively. Gain Rm can be represented using a single-pole model that is given by equations 3.3 & 3.4. OTRA can be used in simple open loop setup. The increase in output voltage however, is nevertheless infinite that saturates at the positive or negative saturation level. Open loop application of OTRA is shortened. So in general OTRA is used in closed-loop configuration with negative feedback to avoid driving into saturation and to work in the linear region. Since it's a transresistance amplifier shunt-shunt feedback is adopted. Feedback configuration

of OTRA has a vast area of application because bandwidth becomes almost independent of closed-loop gain after employing current feedback techniques.

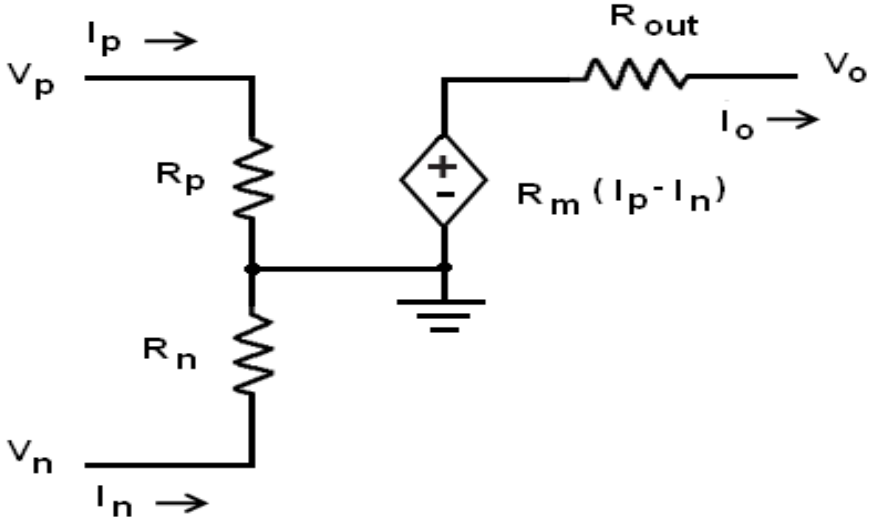

Fig 3.3 Equivalent circuit model of practical OTRA

For a practical OTRA R_m can be expressed mathematically as

$$R_m(S) = \frac{R_0}{1+{}^{S}/_{\omega_0}} \tag{3.3}$$

where R_o is DC open loop transresistance gain. For high frequency applications, the transresistance gain, Rm (s) can be expressed as

$$R_m(S) \approx \frac{R_0}{{}^{S}/_{\omega_0}} = \frac{1}{{}^{S}/_{R_0\omega_0}} = \frac{1}{SC_p} \tag{3.4}$$

Where "C_p" is the parasitic or stray capacitance of OTRA which is unwanted and is unavoidable. Circuits that operate in low frequency, the value of parasitic capacitance is so less that can be ignored but circuits with high frequency, it can be a major problem. With type of applications it can form a feedback path between input and output resulting in oscillations. Such kind of oscillations is called parasitic oscillations. In fact combining with stray inductance, parasitic capacitance may lead circuits to resonate at high frequency.

3.2 IMPLEMENTATION OF OTRA USING CMOS

In this chapter implementation of OTRA is discussed. A comprehensive review shows a number of implementations of OTRA. However it can be broadly classified into two types: OTRA using CFOA and OTRA using CMOS.

As CMOS has very little static power dissipation, high noise margin, lower area requirement, designers opt for CMOS circuit realizations. This section describes implementation of OTRA[37] that is used to verify the functionality of all the circuit structures of this thesis.

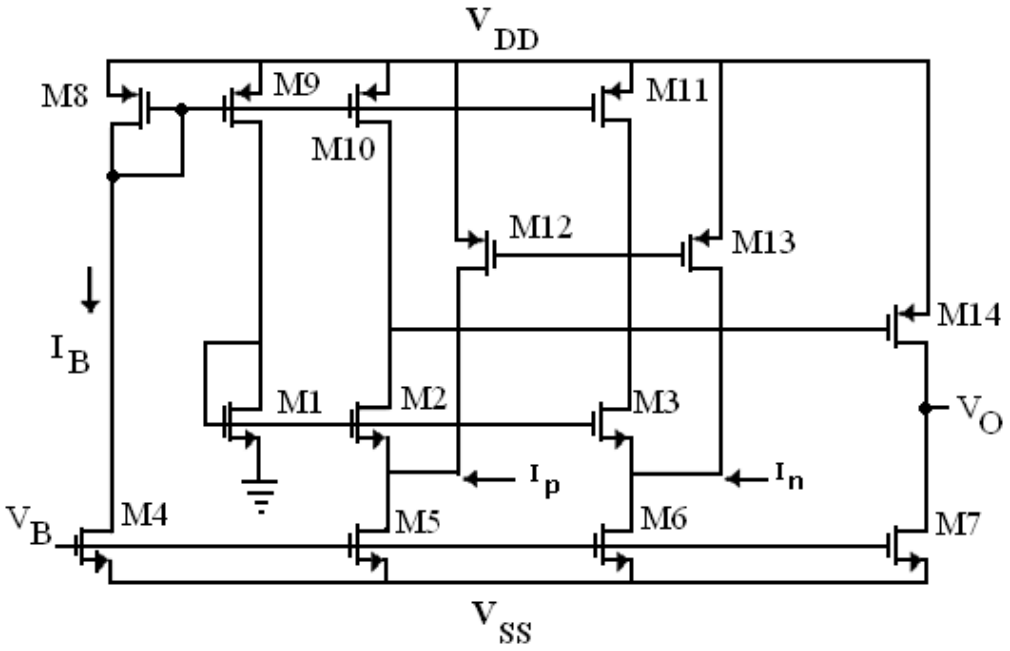

Fig 3.4 CMOS OTRA[37]

The circuit can be explained as follows. There are total 14 transistors including seven PMOS and seven NMOS. Transistor groups [M1-M3], [M5-M6], [M8-M11] and [M12-M13] should be perfectly matched. It is assumed that all the transistors operate in saturation mode so that current can be maximum. The current biasing I_B is connected to the transistors M8 with common gate and thus biases the transistors M8 to M11. The

current mirror which is formed by transistors M8 to M11 pushes equal current flowing through transistors M1, M2 & M3. Thus gate to source voltage of transistors M1, M2 & M3 becomes equal and consequently compels the two input terminals to be virtually grounded. The current mirrors made by the transistor pairs M10-M11 & M12-M13 provide the current differencing operation and produces gate to source voltage for transistor M14 that is connected as common source amplifier and therefore offers high gain to the output.

3.2.1 SIMULATION RESULT

The circuit of Fig.3.4 has been simulated on PSPICE using the TSMC 180nm process parameters, given in table 3.1. Supply voltages for simulation are taken as $\pm 1.5V$ and biasing current I_B = 23µA and biasing voltage V_B = -0.5V are used. Aspect ratios of different MOSFETs[37] are listed in table 3.2.

Table 3.1 Aspect ratios

Transistor	W(µm)/L(µm)
M1-M3	100/2.5
M4	10/2.5
M5,M6	30/2.5
M7	10/2.5
M8-M11	50/2.5
M12,M13	100/2.5
M14	50/0.5

Table 3.2 Device Model Parameters

Device type	Model Parameters
PMOS	+VERSION = 3.1 TNOM = 27 TOX = 4.1E-9 +XJ = 1E-7 NCH = 4.1589E17 VTH0 = -0.4045149 +K1 = 0.5513831 K2 = 0.0395421 K3 = 0 +K3B = 5.7116064 W0 = 1.003172E-6 NLX = 1.239563E-7 +DVT0W = 0 DVT1W = 0 DVT2W = 0 +DVT0 = 0.6078076 DVT1 = 0.2442982 DVT2 = 0.1 +U0 = 116.1690772 UA = 1.536496E-9 UB = 1.17056E-21 +UC = -9.96841E-11 VSAT = 1.324749E5 A0 = 1.9705728 +AGS = 0.4302931 B0 = 2.927795E-7 B1 = 6.182094E-7 +KETA = 2.115388E-3 A1 = 0.6455562 A2 = 0.3778114 +RDSW = 168.4877597 PRWG = 0.5 PRWB = -0.4990495 +WR = 1 WINT = 0 LINT = 3.029442E-8 +XL = 0 XW = -1E-8 DWG = -3.144339E-8 +DWB = -1.323608E-8 VOFF = -0.1008469 NFACTOR = 1.9293877 +CIT = 0 CDSC = 2.4E-4 CDSCD = 0 +CDSCB = 0 ETA0 = 0.0719385 ETAB = -0.0594662 +DSUB = 0.7367007 PCLM = 1.0462908 PDIBLC1 = 2.709018E-4 +PDIBLC2 = 0.0326163 PDIBLCB = -1E-3 DROUT = 9.231736E-4 +PSCBE1 = 1.060432E10 PSCBE2 = 3.062774E-9 PVAG = 15.0473867 +DELTA = 0.01 RSH = 7.6 MOBMOD = 1 +PRT = 0 UTE = -1.5 KT1 = -0.11 +KT1L = 0 KT2 = 0.022 UA1 = 4.31E-9 +UB1 = -7.61E-18 UC1 = -5.6E-11 AT = 3.3E4 +WL = 0 WLN = 1 WW = 0 +WWN = 1 WWL = 0 LL = 0 +LLN = 1 LW = 0 LWN = 1 +LWL = 0 CAPMOD = 2 XPART = 0.5 +CGDO = 6.54E-10 CGSO = 6.54E-10 CGBO = 1E-12 +CJ = 1.154124E-3 PB = 0.8414529 MJ = 0.406705 +CJSW = 2.50766E-10 PBSW = 0.8 MJSW = 0.3350647 +CJSWG = 4.22E-10 PBSWG = 0.8 MJSWG = 0.3350647 +CF = 0 PVTH0 = 2.252845E-3 PRDSW = 7.5306858 +PK2 = 1.57704E-3 WKETA = 0.0355518 LKETA = 7.806536E-3 +PU0 = -1.6701992 PUA = -5.63495E-11 PUB = 1E-21 +PVSAT = 49.8423856 PETA0 = 9.968409E-5 PKETA = -3.957099E-3 *
NMOS	+VERSION = 3.1 TNOM = 27 TOX = 4.1E-9 +XJ = 1E-7 NCH = 2.3549E17 VTH0 = 0.3932664 +K1 = 0.5826058 K2 = 6.016593E-3 K3 = 1E-3 +K3B = 1.4046112 W0 = 1E-7 NLX = 1.755425E-7 +DVT0W = 0 DVT1W = 0 DVT2W = 0 +DVT0 = 1.3156832 DVT1 = 0.397759 DVT2 = 0.0615187 +U0 = 280.5758609 UA = -1.208176E-9 UB = 2.159494E-18 +UC = 5.340577E-11 VSAT = 9.601364E4 A0 = 1.7852987 +AGS = 0.4008594 B0 = -3.73715E-9 B1 = -1E-7 +KETA = -1.136459E-3 A1 = 2.580625E-4 A2 = 0.9802522 +RDSW = 105.472458 PRWG = 0.5 PRWB = -0.2 +WR = 1 WINT = 0 LINT = 1.571909E-8 +XL = 0 XW = -1E-8 DWG = -7.918114E-9 +DWB = -3.223301E-9 VOFF = -0.0956759 NFACTOR = 2.4447616 +CIT = 0 CDSC = 2.4E-4 CDSCD = 0 +CDSCB = 0 ETA0 = 2.489084E-3 ETAB = -2.143433E-5 +DSUB = 0.0140178 PCLM = 0.7533987 PDIBLC1 = 0.1966545

	+PDIBLC2 = 3.366782E-3 PDIBLCB = -0.1 DROUT = 0.7760158 +PSCBE1 = 8E10 PSCBE2 = 9.204421E-10 PVAG = 5.676338E-3 +DELTA = 0.01 RSH = 6.5 MOBMOD = 1 +PRT = 0 UTE = -1.5 KT1 = -0.11 +KT1L = 0 KT2 = 0.022 UA1 = 4.31E-9 +UB1 = -7.61E-18 UC1 = -5.6E-11 AT = 3.3E4 +WL = 0 WLN = 1 WW = 0 +WWN = 1 WWL = 0 LL = 0 +LLN = 1 LW = 0 LWN = 1 +LWL = 0 CAPMOD = 2 XPART = 0.5 +CGDO = 7.83E-10 CGSO = 7.83E-10 CGBO = 1E-12 +CJ = 9.969364E-4 PB = 0.8 MJ = 0.376826 +CJSW = 2.618614E-10 PBSW = 0.8321894 MJSW = 0.1020453 +CJSWG = 3.3E-10 PBSWG = 0.8321894 MJSWG = 0.1020453 +CF = 0 PVTH0 = -1.428269E-3 PRDSW = -4.3383092 +PK2 = 8.440537E-5 WKETA = 2.341504E-3 LKETA = -9.397952E-3 +PU0 = 15.2496815 PUA = 5.74703E-11 PUB = 1.593698E-23 +PVSAT = 857.5761302 PETA0 = 1.003159E-4 PKETA = -1.378026E-3

In Fig 3.5 DC Transfer characteristics is shown. Output voltage is plotted against input current I_p keeping I_n constant (at 0A). By performing the same for I_n, similar curve is found. From Fig. 3.5 input differential range can be found as -50µA to +50µA. Input impedance is plotted in Fig. 3.6. Actually it is the open loop gain of OTRA measured in units of ohms and then taken log on it.

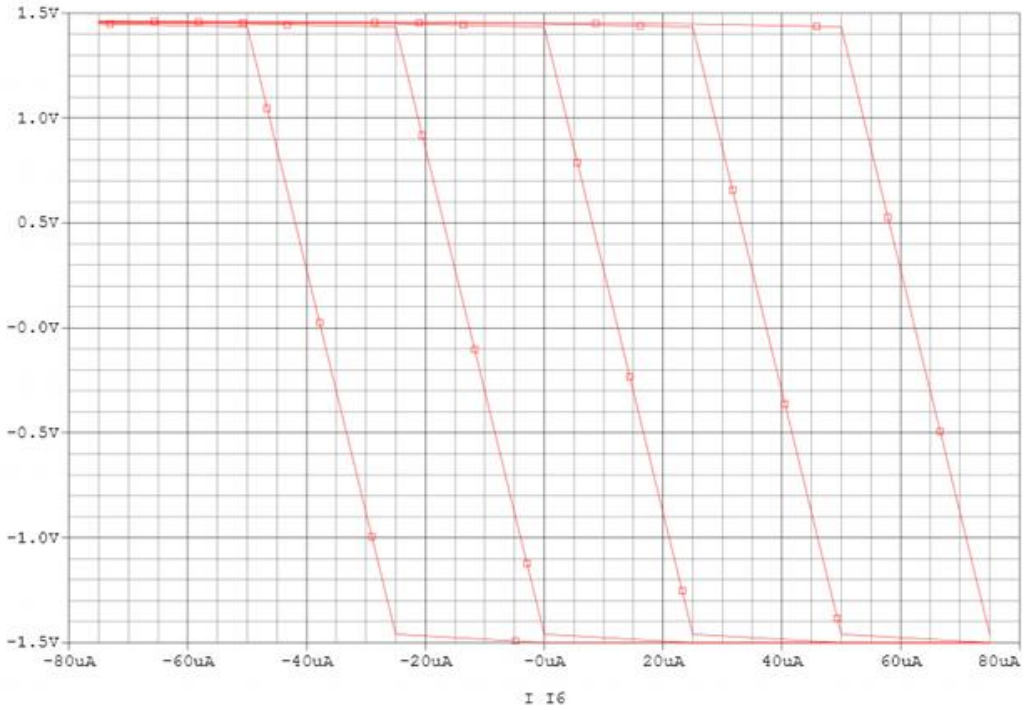

Fig. 3.5 DC Transfer characteristics of OTRA

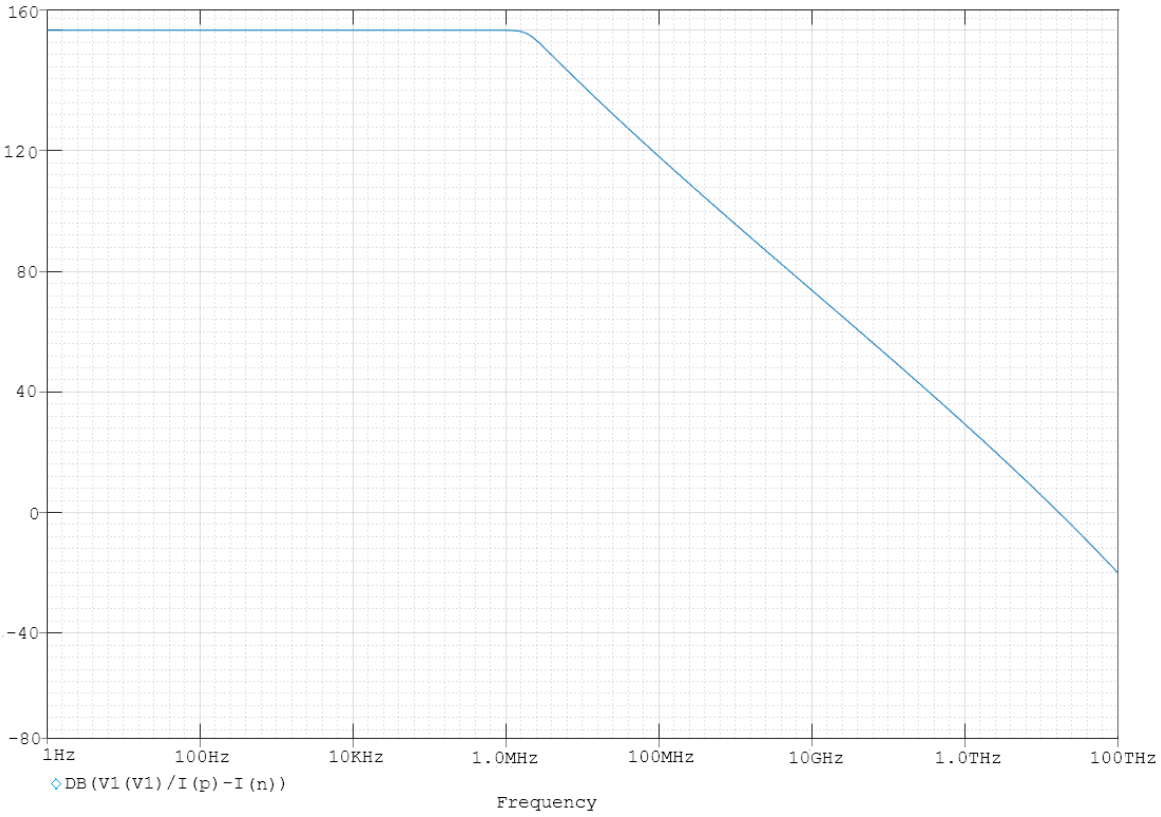

Fig. 3.6 Open Loop Gain of OTRA

From Fig. 3.6, frequency equals 104MHz, so gain R_m will be

$R_m = 20\log_{10}(10 \times 10^6)\ dB\Omega$

$\approx 160.34\ dB\Omega$

CHAPTER 4

SINUSOIDAL OSCILLATOR USING OTRA

4.1 INTRODUCTION

A function or signal generator is a kind of device which is used to produce signals with different shapes, frequencies, duty cycles etc**.** An oscillator is a kind of signal generator that can produce continuous, repeating alternate waveforms without employing any input. They find numerous applications in communication, instrumentation, control and measurement systems. From producing periodic signals like sine wave, pulse train, sawtooth, triangular wave etc to testing any circuits, waveform generators find extensive applications. The LC tanks are the first invented circuit to produce sinusoidal oscillations. However in an LC tank circuit there are losses in the coil (resistive & radiation) and dielectric loss in the capacitor resulting in damped oscillation. A transistor amplifier with proper positive feedback can act as an oscillator where the oscillation is sustained by feeding back a fraction of the output signal. Positive feedback requires a part of the output to be in phase with the input. The basic principle behind the working of an oscillator is to convert direct current from power supply into alternating current. Oscillation is an effect that repeatedly and regularly fluctuates about the mean value.An oscillator is characterized by its oscillation amplitude (or power), frequency, "stability", phase noise, and tuning range. An oscillator is said to be stable if its frequency and amplitude of oscillation do not vary appreciably with temperature, process parameters, power supply, and external disturbances[38].

Oscillators can be broadly classified as

1. Harmonic/ Sinusoidal/ linear oscillators
2. Non-linear/ Relaxation oscillators.

The functional block diagram of sinusoidal oscillator with positive feedback[39] is shown in Fig. 4.1

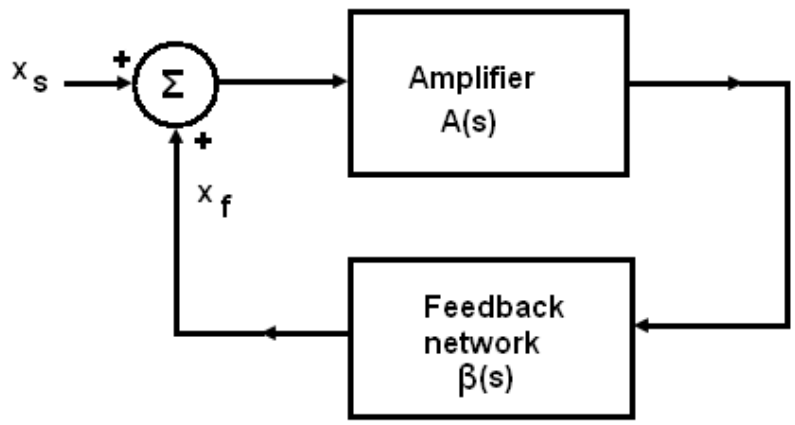

Fig. 4.1 Functional block diagram of oscillator[39]

A(S) and β(S) are the gains of amplifier and feedback network respectively. X_S and X_f are the input and feedback signals, whereas Y_S is the output signal. The closed loop transfer function of the block diagram shown in Fig. 4.1 becomes

$$\frac{Y(S)}{X(S)} = \frac{A(S)}{1-A(S)\beta(S)} \tag{4.1}$$

Thus the characteristic equation can be written as,

$$1 - A(S)\beta(S) = 0 \tag{4.2}$$

According to Barkhausen criterion, the system will sustain steady state oscillations at a specific frequency only when the open-loop gain is equal to unity, thus

$$A(S)\beta(S) = 1 \tag{4.3}$$

At this condition, the closed-loop gain becomes infinite and produces a finite output for the zero input signals. The Barkhausen criterion is widely used in designing electronic oscillators and also in the design of the feedback circuits to prevent them from oscillations.

4.2 REALIZATION OF OSCILLATOR USING OTRA

In this section an OTRA based oscillator[40] is implemented. This oscillator uses three resistors of equal value and three capacitors. It uses grounded capacitance and provides independent control of its oscillating frequency. Due to presence of grounded capacitors, it can easily filter out unwanted signals and provide excellent performance in high, low or medium frequency applications.The output impedance of this oscillator is low and therefore cascading with other circuits becomes easier.

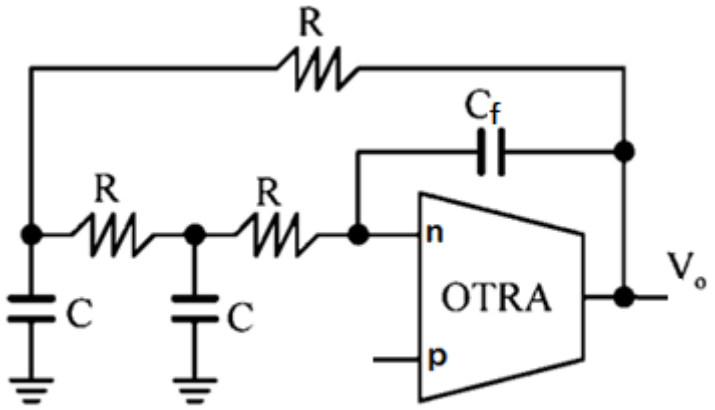

Fig. 4.2 Oscillator using OTRA[40]

The charecteristic equation of the above circuit can be found as

$$S^3R^3C^2C_f + S^2 4R^2CC_f + S3RC_f + 1 = 0 \quad (4.4)$$

From equation (4.4) condition of oscillation(CO) can be found as

$$C \leq 12C_f \tag{4.5}$$

$$C_f \geq {}^{C}/_{12} \tag{4.6}$$

For critical oscillation, $C = 12C_f$ (4.7)

Equation (4.5) follows Barkhausen criteria for theoritical analysis but in practical it gives damped oscillation, so for all practical circuits 'C' should be taken slightlty greater than '$12C_f$' to start oscillation and to avoid decaying of desired output after a certain time.

From equation (4.4), frequency of oscillation(FO) can be given as,

$$\omega_0 = \frac{\sqrt{3}}{RC} \tag{4.8}$$

Where, $\omega_0$is the angular frequency. In terms of Hz, FO equals,

$$f_0 = \frac{\sqrt{3}}{2\pi RC} \tag{4.9}$$

From equation (4.5) and (4.8) we can see that this oscillator has an independent control over FO & CO.

While deriving the characteristic equation , OTRA is considered to be ideal i.e. it has no paracitic capacitance even in high frequency applications. However practically this is not possible.

4.2.1 NON-IDEALITY ANALYSIS

In high frequency applications of OTRA, there comes a capacitance called parasitic or stray capacitance(C_p) due to different electric charges present at different parts of the circuit when they are in close proximity. C_p is unwanted and unavoidable. Considering nonideal characteristics of OTRA characterisctic equation of the oscillator would be modified as,

$$S^3\{R^3C^2(C_p + C_f)\} + S^2\{4R^2C(C_p + C_f)\} + S\{3R(C_p + C_f)\} + 1 = 0 \tag{4.10}$$

Where, C_p and C_f are the parasitic and feedback capacitance respectively.

From equation 4.2.2 condition of oscillation can be given as

$$C \leq 12(C_p + C_f) \tag{4.11}$$

For critical oscillation,

$$C = 12(C_p + C_f) \tag{4.12}$$

4.2.2 SENSITIVITY ANALYSIS

It is important to know the sensitivities of circuits with respect to its components variation. For this oscillator sesitivity of frequency with respect to resistance(R) can be derived as,

$S_R^{\omega_0} = \frac{R}{\omega_0} \times \frac{d\omega_0}{dR}$, keeping 'C' constant

$= \frac{R}{\sqrt{3}/_{RC}} \times \frac{d}{dR}\left[\frac{\sqrt{3}}{RC}\right]$, using equation (4.8)

$= \frac{R^2C}{\sqrt{3}} \times \left[\frac{-\sqrt{3}}{R^2C}\right]$

$= -1$

Similarly sensitivity with respect to capacitance, C while 'R' is constant can be given as,

$S_C^{\omega_0} = -1$

So this circuit offers low parameter sensitivity to its frequency which is crucial for good perfomance.

4.2.3 SIMULATION RESULT

The functionality of the oscillator of Fig. 4.2 is verified by PSpice simulation using CMOS OTRA[37] as discussed in 3.2.2. During implementation, TSMC 180nm CMOS process parameters were adopted. Supply voltage of ±1.5V and biasing current of 25µA are taken and C & R are varied to get desired response.

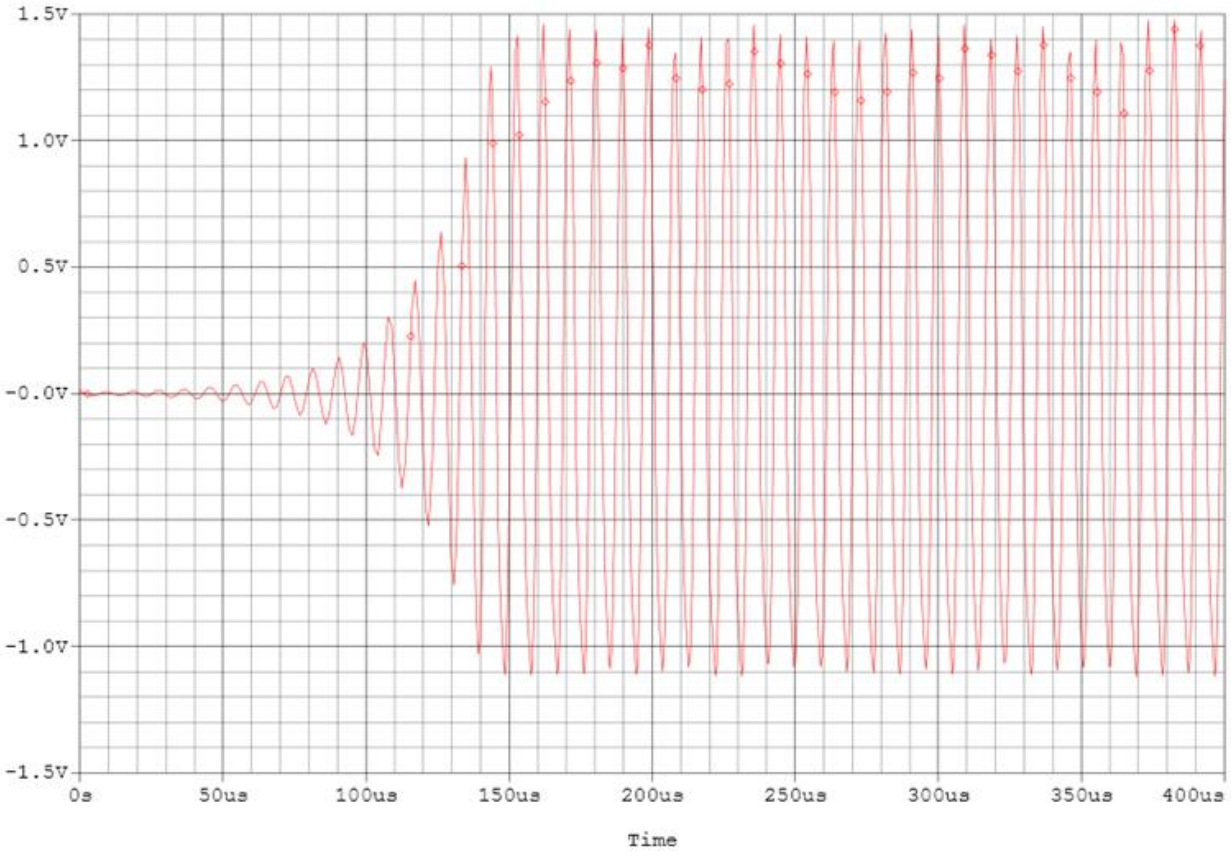

Fig. 4. 3 Start-up oscillation of the oscillatior, f_0=112KHz, R = 220Ω, C_f = 0.9nF, C=12.1nF

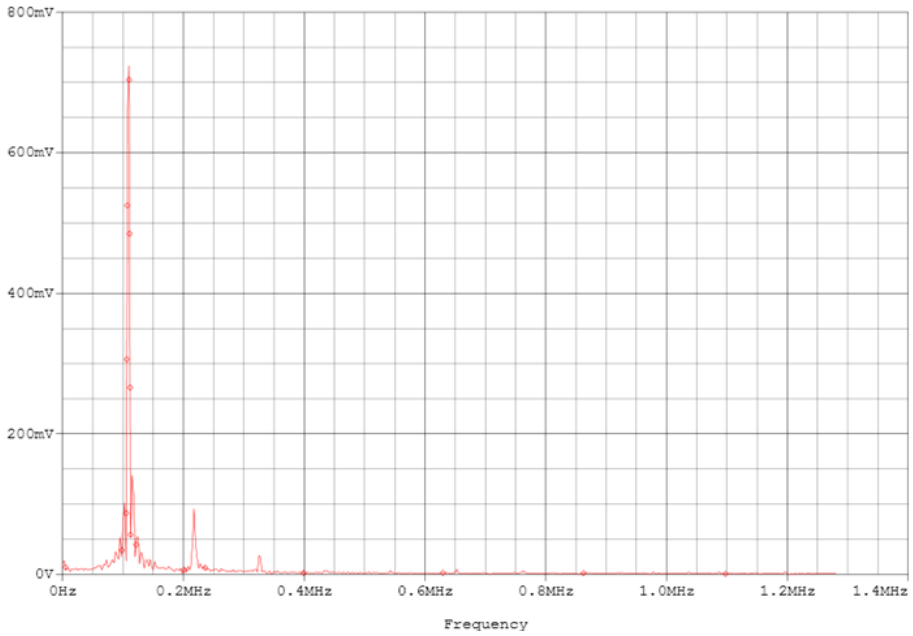

Fig. 4.4 FFT of start up oscillation

From the graph we can see that the centre frequency of the oscillator is 112KHz. Due to noise a real oscillator does not have an exact delta function power spectrum, rather a very sharp centre frequency.

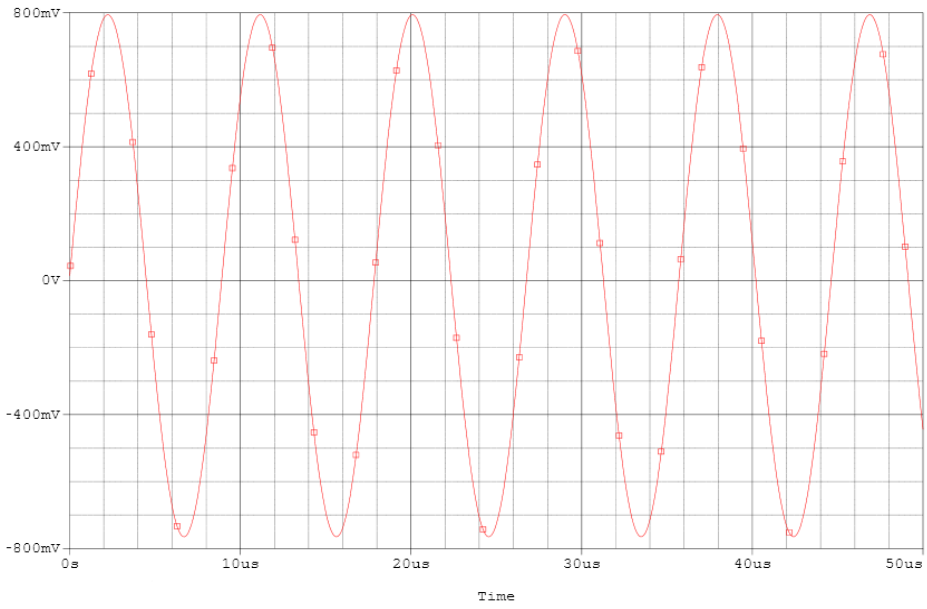

Fig.4.5 Steady state oscillation when f_0=102KHz,
R=227Ω, C=12.1nf, C_f=0.9nF

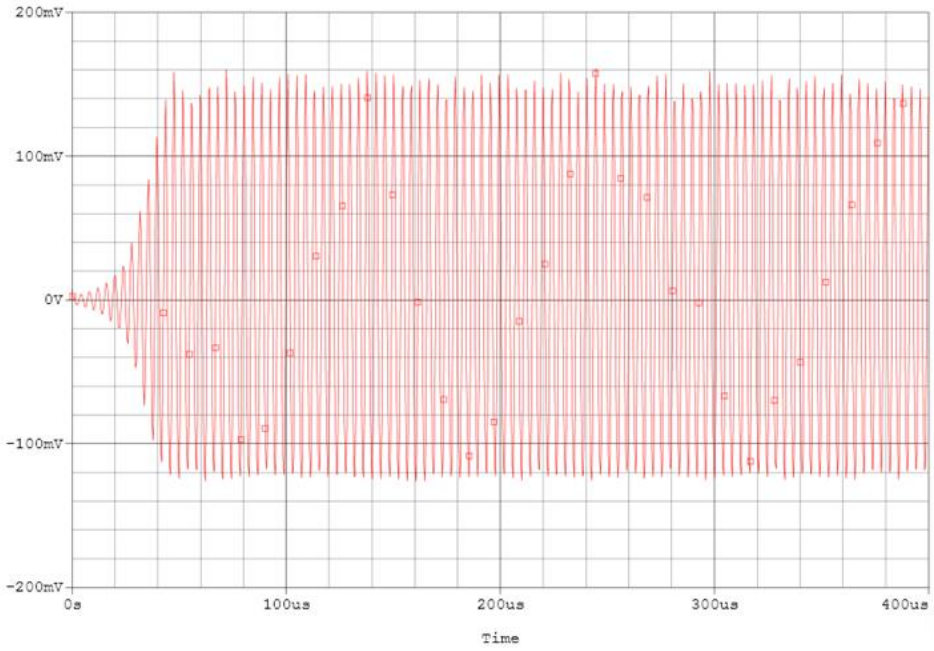

Fig. 4.6 highest applicable oscillations, when f_0=1.25MHz, R=30Ω, C=8nf, C_f=0.9nF

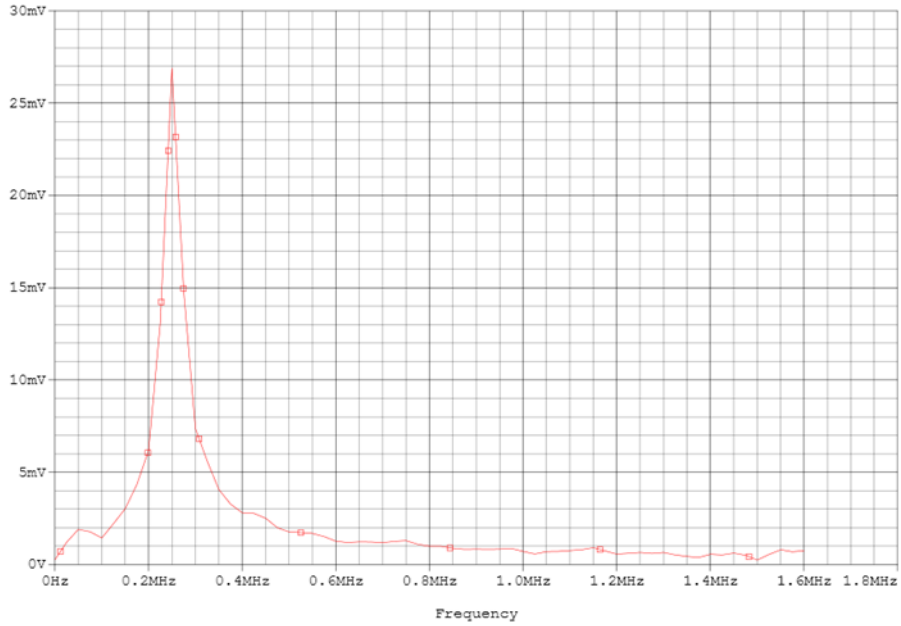

Fig. 4.7 FFT of highest applicable oscillations

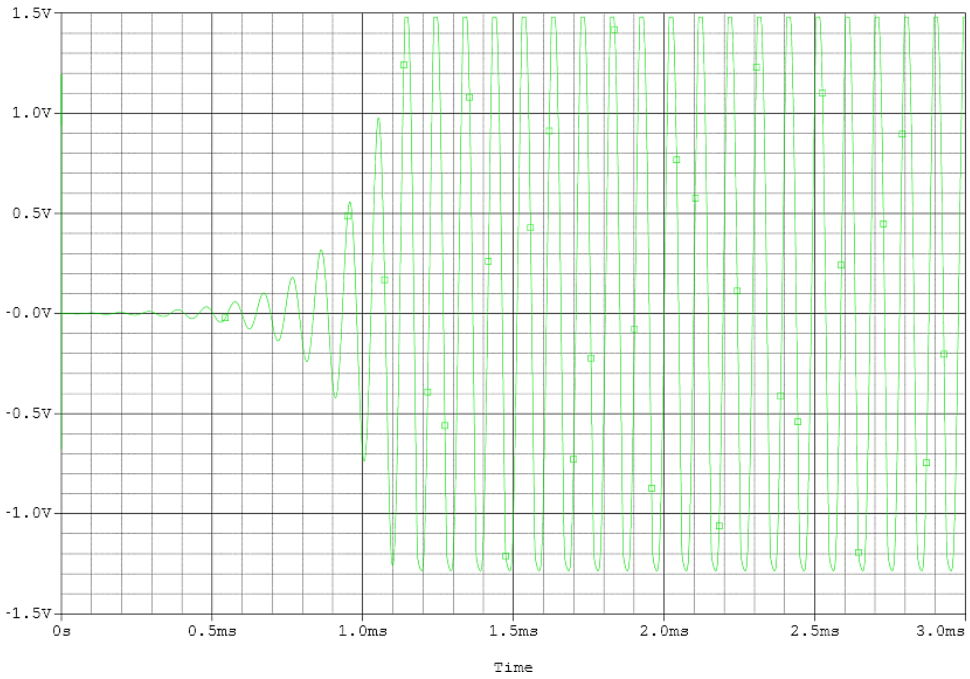

Fig. 4.8 lowest applicable oscillations, when f_0=118KHz, R=1.13KΩ, C=12.1nf, C_f=0.9nF

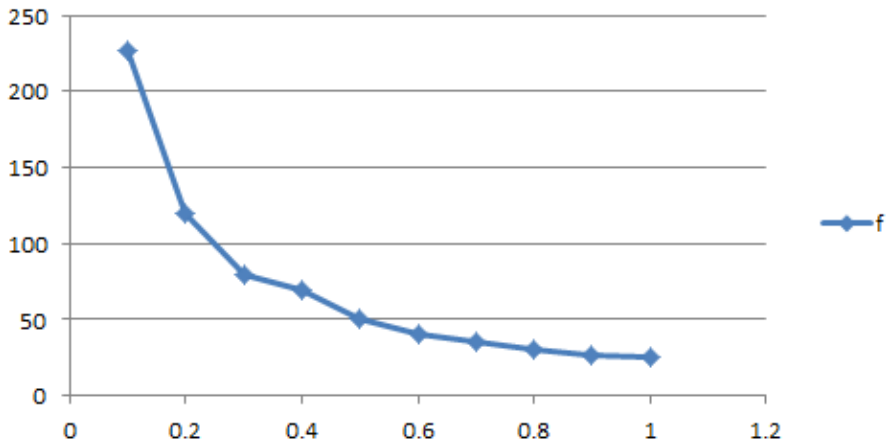

Fig. 4.9 Variation of oscillation frequency(KHz) with resistance(KΩ), keeping capacitance constant

The above figure shows that as resistance increases frequency of oscillation decreases and we get almost DC signal at the output. This figure conveys that tuning of oscillation frequency can be done without affecting oscillation condition. Range of frequency of oscillator of Fig.4.2 is so wide and it goes to some MHz.

Table 4.1 Comparison between implementations using 350nm and 180nm

characteristic	**350nm**	**180nm**
Supply voltage	±2.5V	±1.5V
Biasing current	30µA	25µA
Frequecny, f_0	C_f = 1nF, C=12.1nF, R=227Ω	C_f = 0.9nF, C=12.1nF, R=227Ω
THD when f_c varies from 10KHz to 100KHz	0.91 to 1.93	1.23 to 2.59
Total power consumption	6.8mW	4.42mW

Thus with a reduction of supply voltage decreases the total power consumption and enables its uses in low power electronic systems. Table 4.3.2 shows the details of components and resultant frequencies.

Table 4.2 Details of components and results

Componenet values(C_f = 0.6nF)	**Oscillation frequency(f_0)**		**THD**	**Remarks**
	Theoretical(Hz)	**Experimental(Hz)**		
C=12.1nF, R=1.13kΩ	2K	1.18K	1.23%	Low frequency of oscillaction
C=12.1nF, R=227Ω	100K	102K	1.29%	Mid frequency of oscillation
C=8nF, R=30Ω	1.14M	1.25M	2.1%	High frequency

With a wide range of oscillation frequency(few KHz to some MHz) and freely control over it, this oscillator proves its usefulness in industrial and communication systems.

4.3 QUADRATURE PHASE SINUSOIDAL OSCILLATOR

A quadrature oscillator(QO) generates two single frequency output with equal amplitude and quadrature in phase [41]. The simplest way to change the phase of any signal is to integrate or differentiate that signal when it's a sinusoid. Ideally resultant of both the cases should be 90º out of phase but practically we would not get exact 90º phase shifting. This OTRA based QO has lower components count and better integration and simple circuitry. QOs are extensively used in power electronics, communication and signal processing.

4.3.1 INTEGRATOR

A device that performs integration of its input can be called as an integrator. To generate output, an integrator accumulates the input over a given period of time. In signal processing, an electronic integrator is widely used as a low pass filter(LPF). Generally a LPF consists of two passive elements and one active element. Due to presence of resistor in the feedback path there is a loss of gain in the output

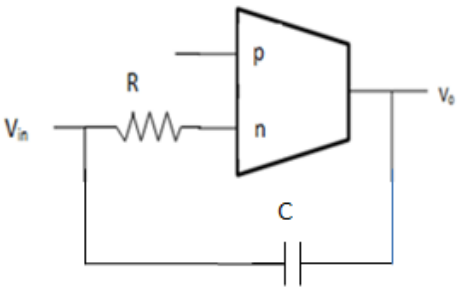

Fig.4.10 Lossless inverting amplifier

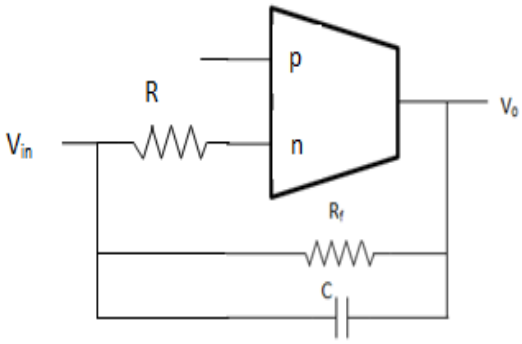

Fig.4.11 Lossy inverting amplifier

Transfer function of integrator in Fig (4.11) can be given as,

$$\frac{V_0}{V_{in}} = \frac{-R_f/R}{1+SCR} \tag{4.13}$$

And DC gain, K = $\frac{-R_f}{R}$ (4.14)

3db frequency of both the integrators will be, $w_0 = \frac{1}{CR}$

In a similar fashion, transfer function of lossless inverting amplifier of Fig.4.10 can be found as,

$\frac{V_0}{V_{in}} = \frac{1}{SCR}$ (4.15)

4.3.1 GENERATION OF QUADRATURE SINUSOIDAL OSCILLATOR

There are various methods to generate quadrature sinusoidal signal. The basic principle is to generate a sine signal and then change its phase by 90°. For this one low pass filter feedbacked with an inverting integrator[41] works fine. Another popular way is to make an oscillator and then cascade it with an integrator. The latter scheme is realized in this chapter. Fig. 4.12 shows block diagram of QO.

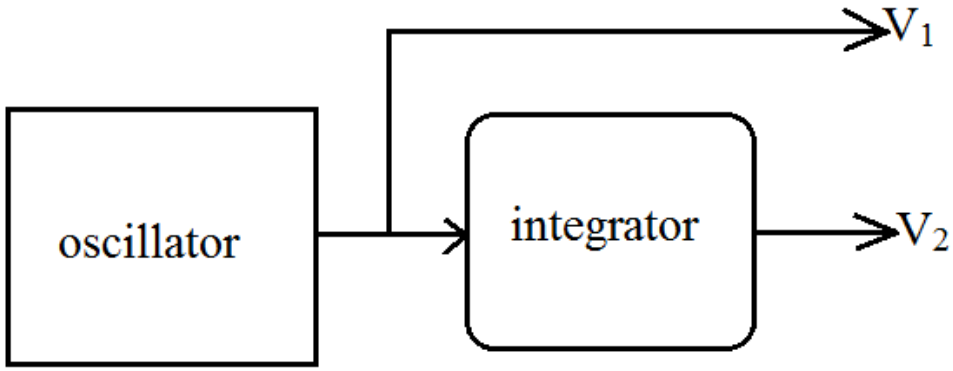

Fig. 4.12 Block diagram of QO

From equation (4.4) we have already got the characteristic equation of oscillator,

$S^3R^3C^2C_f + S^24R^2CC_f + S3RC_f + 1 = 0$

CO: $C \leq 12C_f$

FO:$f_0 = \frac{\sqrt{3}}{2\pi RC}$

After cascading an integrator, the output signal will be shifted by 90°out of phase but frequency remains same. So CO & FO will be same as it was for the main oscillator.

4.3.2 IMPLEMENTATION OF QO

QO is implemented using Pspice and TSMC 180nm parameter files. Fig. 4.13 depicts the circuit diagram QO. Supply voltages & biasing currents remain same(±1.5V & 25μA).

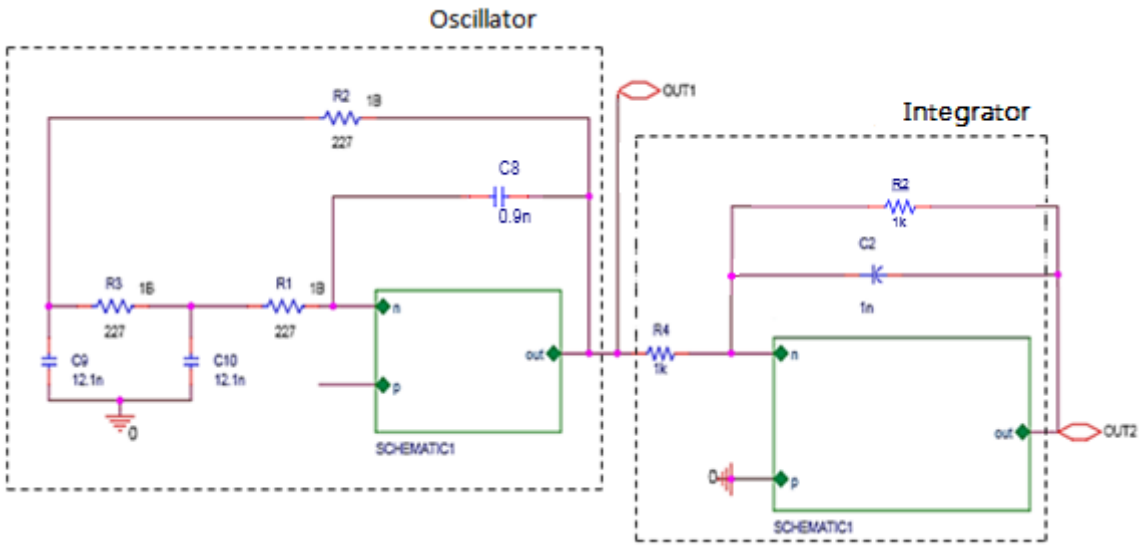

Fig. 4.13 Circuit Diagram of QO

Table 4.3 Component details of OTRA based QO with supply voltage = ±1.5V

Name of the subcircuit	Component values
Oscillator	C_f =0.9nF, C=12.1nF, R=227Ω
Integrator	C=1nF, R=1KΩ

4.3.3 SIMULATION RESULT

After simulating the circuit of Fig.4.13 we get two sinusoidal signals with same frequency and 90° phase difference. The oscillator is designed to work at 115KHz by selecting the component values as C=12.1nF, R=198Ω. The simulated FO is found to be 117KHz.So there is a slight variation from theritical value, precisely 1.73%. THD wass found 2.6%. Outputs of QO are shown in the below figures:

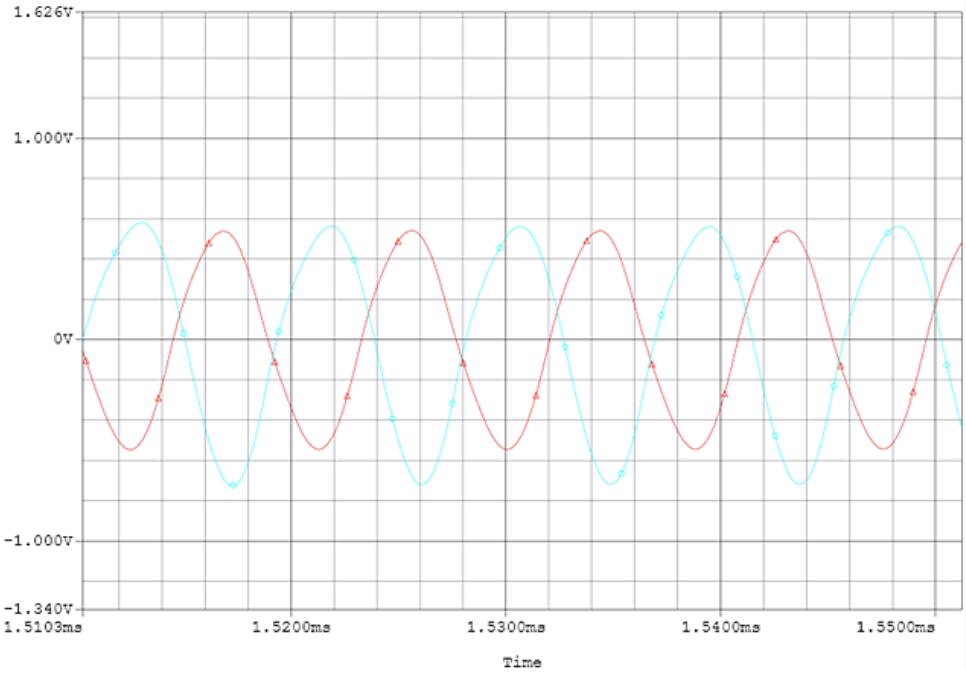

Fig. 4.14 QO output

The graph shown above represents two sinusoidal waves with almost eual magnitude and 90° phase difference. Slight difference in amplitude comes due to presence of internaal parasitic capacitances of the integrator.

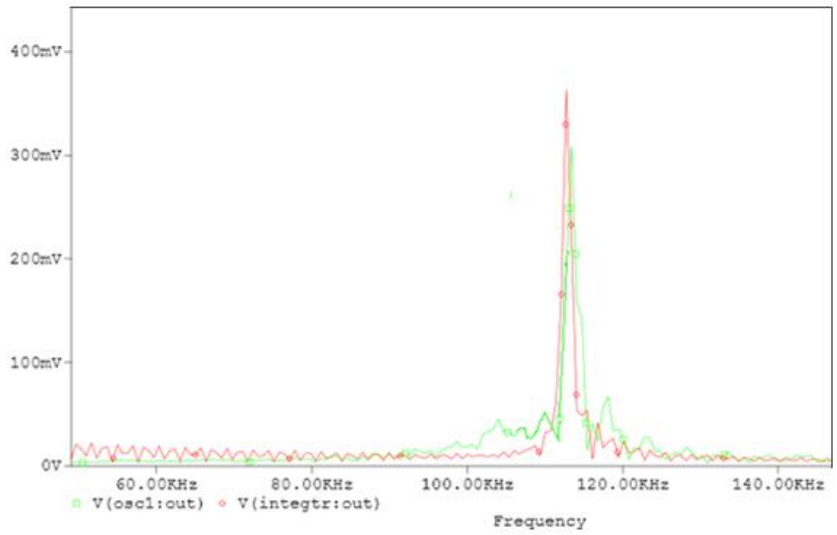

Fig. 4.15 Frequency spectrum of QO output

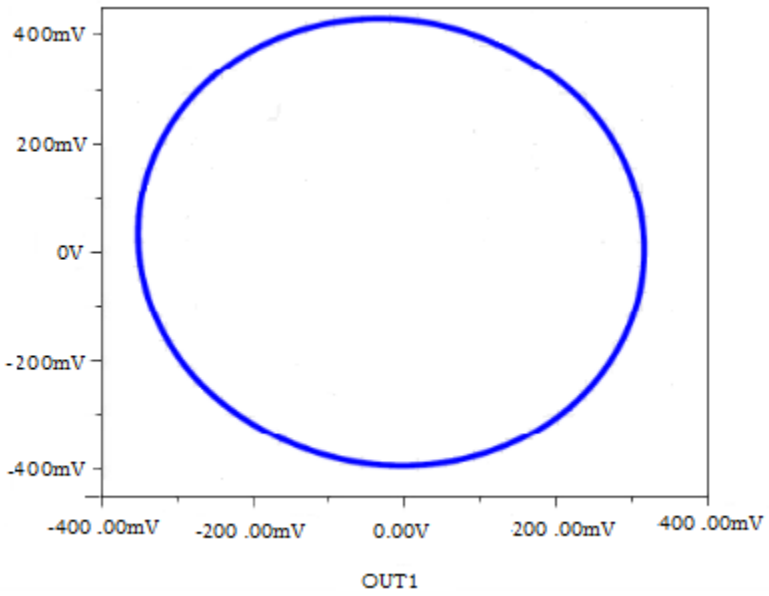

Fig. 4.16 V1 vs V2 graph

Thus the above two graphs depict almost perfect QO output with same frequency and almost 90° phase difference.

APPLICATION OF OTRA BASED CIRCUITS IN THE FIELD OF COMMUNICATION

Essentially the word “communication” means sharing or exchanging information between two (or more) individuals or systems. A communication system is a collection of elements that work together to set up a bridge between the sender and the receiver. Any communication system[45] has three major parts: sender, channel & receiver. Transmitter sends the data or message and might be called as communicator or source of information. Channel is the medium through which message signal travels from transmitter to the receiver and then the job of the receiver is to receive the signal properly. However practically it is not that simple since there are vast types of signals and they have to travel a very long distance. In general signals need to be transformed into electrical one before transmitting. Input transducers are used for this purpose. After that signals need to be modulated before reaching to transmitter. The block diagram of any general communication system is shown in fig.5.1:

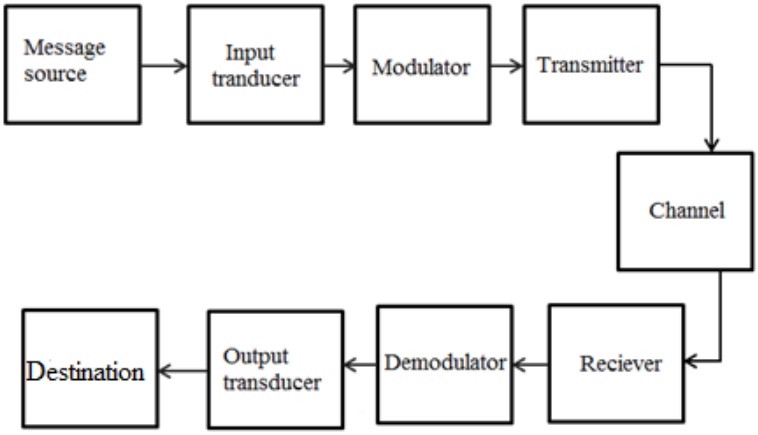

Fig. 5.1 Communication System

This chapter focuses on designing of various communication modules with the help of OTRA based circuits. Among these oscillator is a crucial part of any communication system. Oscillators are mainly used to generate clocks in digital systems, sweep circuits in TV sets and CRO. In communication systems local oscillators are used to produce RF carrier in the transmitter and transforms RF signals to IF signals in the receiver. Before presenting OTRA based implementation in the following sections basics of analog modulation and demodulation schemes are presented.

5.1 ANALOG MODULATION AND DEMODULATION SCHEMES

Due to its small signal strength, a message signal cannot travel long distances. In addition to this, physical surroundings, presence of external noise further reduce the message signal strength. Therefore we need to raise the signal strength[45] to be sent over a long distance, which can be done by the process of modulation. A high energy signal can pass a wider range without getting affected by external disturbances. The signal of high energy or high frequency is called 'carrier signal' and the process is known as 'modulation'. In simple words modulation is embedding a message signal onto a carrier signal or elaborately we can say that modulation is a process of altering the characteristics of carrier wave in accordance with the transmitted message signal (also named as 'modulating signal'). And the result is referred as modulated signal. By the word 'signal' we mean the wave that carries some useful information. In general the frequency of message signal is very low compared to frequency of carrier wave. Frequency range of carrier signal may vary from few KHz to GHz or even more than that. And the message signal is a low frequency signal (few Hz to KHz). We can transmit voice, video or any other kind of data signals and the carrier wave can be AC/DC or pulse train depending on our requirements. When the input signal to the transmitter is analog in nature, it is called 'analog modulation'. Analog signal is a continuous signal whose characteristics like amplitude, voltage or frequency changes continuously over a period of time. To generate carrier wave a local oscillator is used. It is an electronic oscillator used with a mixer to produce signals having different frequencies. The OTRA based sinusoidal oscillator (discussed in 4.2) can be used for this.

In modern communication system modulation is inevitable because it allows making smaller antennas otherwise a low frequency(baseband) signal would demand huge sized antennas in the transmitter. Another vital reason is multiplexing. It is a process in which signals from different sources having different input frequencies can be transmitted simultaneously through a common channel. Signals should not interfere with each other while they are multiplexed and this is possible only if they have a different centre frequency. And to get back original signal at the receiver end we need to demodulate it. Therefore both modulation and demodulation are necessary for any communication system[45]. Modulation can be broadly classified into two types: analog and pulse or digital modulation. Most of the natural signals are analog in nature. Traditional communication systems like AM/FM radios, NTSC TV signals are based on analog modulations, but recent systems like 2G, 3G, 4G cellphones, DSL, HDTV are all digital.

Analog modulation refers to the process of transferring an analog baseband (low frequency) signal like an audio or TV signal over a higher frequency band such as radio frequency. There are two ways to modulate an RF carrier: Amplitude Modulation and Angle Modulation. In analog modulation,the amplitude of the carrier signal is made to follow the amplitude of the message signal. Several variants of amplitude modulation are used in practice. Some of them will be discussed in the next section.

5.1.1 DSB-SC MODULATION

"DSB-SC" stands for Double Side Band Suppressed Carrier[46]. It is a type of amplitude modulation where the carrier is attenuated or suppressed before transmitting the modulated signal through the transmitter. DSBSC modulator is used to transmit message signal via a radio frequency wave. In analog TV for colour transmission, key less remotes, air traffic control radios where two way communications happen DSB-SC finds its utilizations. In this section generation of DSB-SC modulator with only based circuits is presented.

Assume an analog message signal m(t) is to be transmitted through the transmitter. Signal m(t) is low pass in nature and has a bandwidth $2f_m$, where f_m is the message signal frequency. The Fourier Transform of m(t) can be given as

$M(F) = 0, for\ |f| \geq 2f_m$

In the process of modulation carrier signal c(t) is used which is produced by Local oscillator (LO). Mathematically c(t) can be expressed as

$c(t) = A_c Cos(2\pi f_c t)$, assuming that phase of the carrier is 0°

A_c is the carrier amplitude, f_c is the carrier frequency. Both the message and carrier signals are power signals. The block diagram of generation of DSB-SC is shown below:

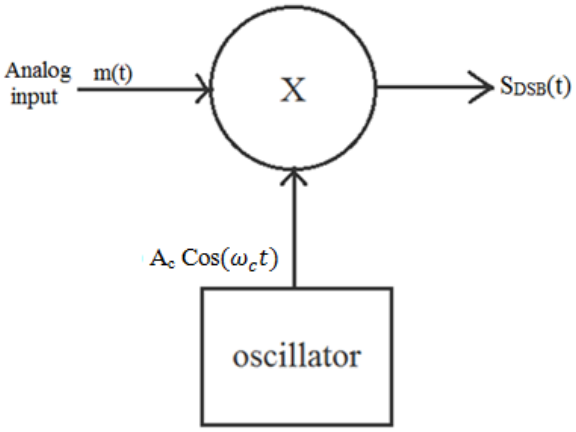

(a)

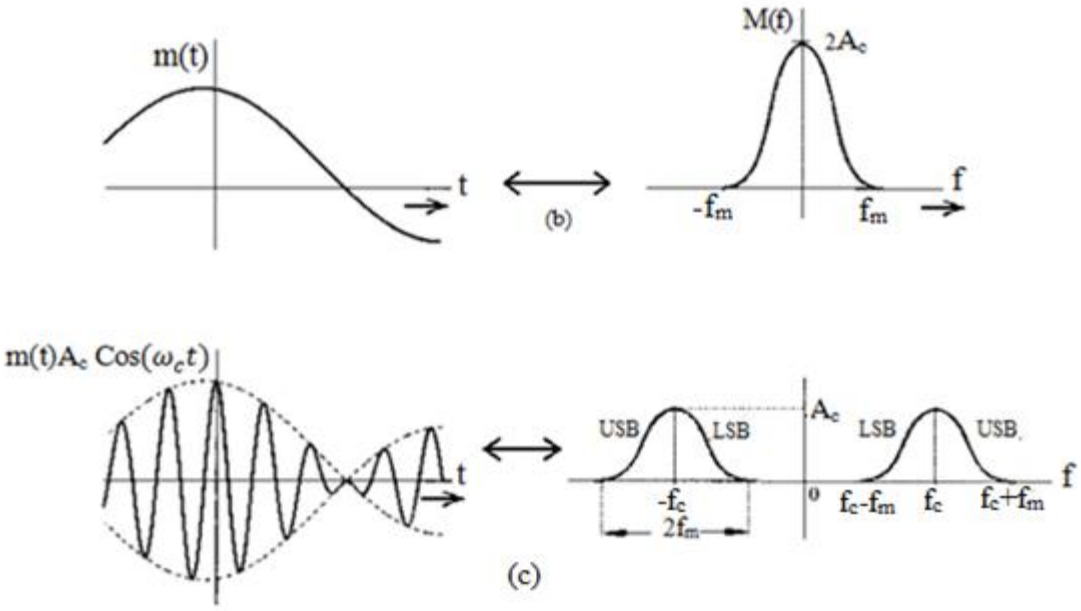

Fig. 5.2 Pictorial representation of DSB-SC modulation : (a) generation (b) message signal and its spectrum (c)modulated signal and its spectrum

Mathematically DSB-SC signal[46] can be expressed as,

$$S_{DSB}(t) = m(t)A_c Cos(w_c t)$$

$$= m(t)A_c Cos(2\pi f_c t)$$

$$= A_c m(t) Cos(w_c t) \quad (5.1)$$

$$S_{DSB}(t) = A_c m(t)\frac{1}{2}\left[e^{j2\pi f_c t} + e^{-j2\pi f_c t}\right] \quad (5.2)$$

$$S_{DSB}(t) = \frac{1}{2}A_c m(t)e^{j2\pi f_c t} + \frac{1}{2}A_c m(t)e^{-j2\pi f_c t} \quad (5.3)$$

After doing Fourier analysis of S(t), we get S(f) in frequency domain as given below:

$$S_{DSB}(f) = \frac{1}{2}A_c M[f_c + f_m] + \frac{1}{2}A_c M[f_c - f_m] \quad (5.4)$$

Where f_m is the message signal frequency as we have already seen. Equation (5.4) shows that our low pass(LP) message signal with frequency f_m has been shifted to a frequency same as carrier's, without changing its bandwidth. That is how modulation can be performed in simplest way with only one analog modulator and an oscillator.

5.1.1.1 DSB-SC Realization Using OTRA Based Circuits

This section presents circuit diagram to generate DSB-SC modulated signal along with all the necessary subcircuits. Oscillator of 4.2 has been used twice to generate both carrier signal and message signal. OTRA based analog multiplier reported in [42] is used to modulate the message signal. Oscillator1of Fig. 5.3 is set to produce 25KHz sinusoid, whereas oscillator2 to 110KHz. Thus we get,

$f_m = 25\text{KHz}$ & $f_c = 110\text{KHz}$

Thus after modulation, spectrum of modulated signal should be present at 135KHz and 85KHz.

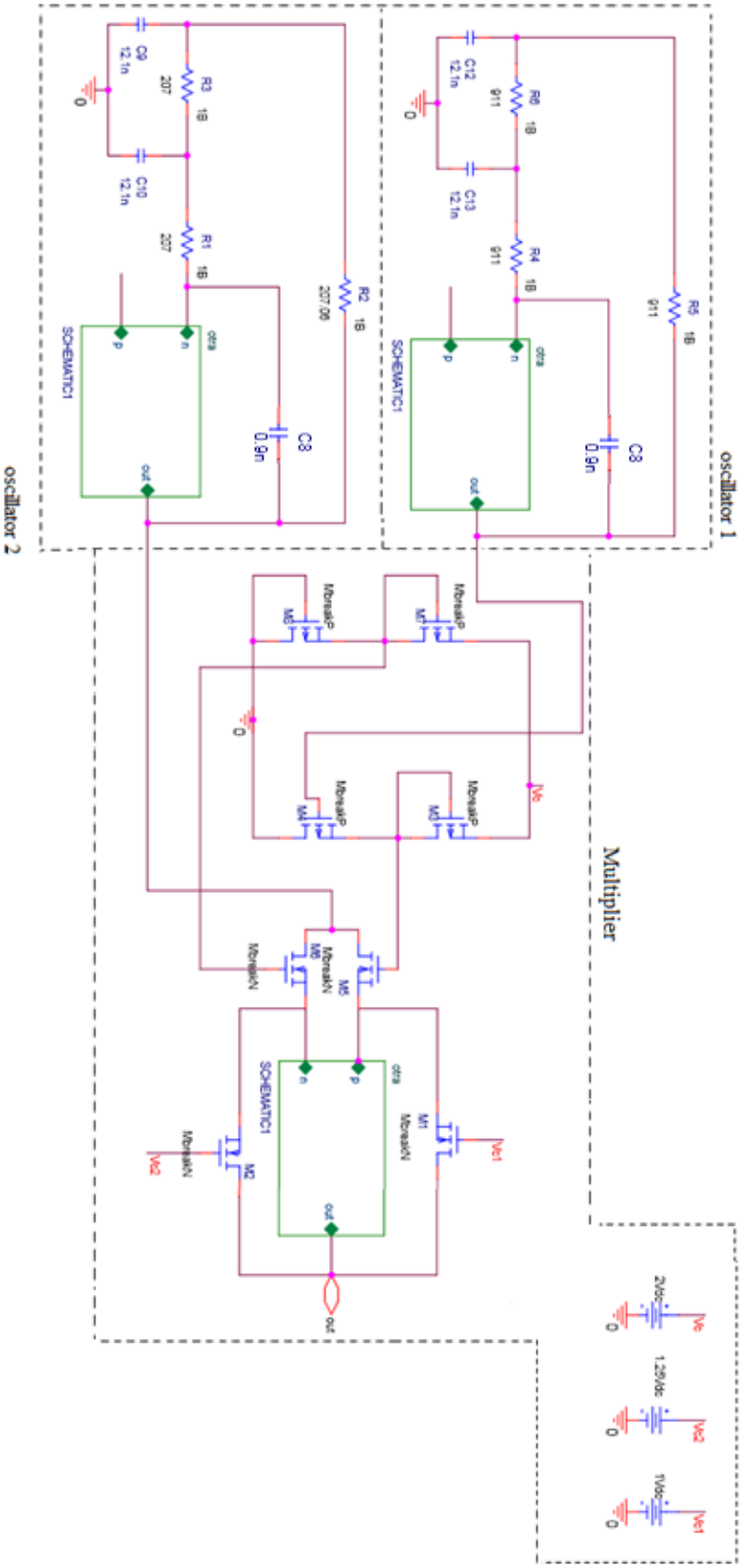

Fig. 5.3 Circuit Diagram of DSB-SC modulator

Table 5.1: Component values used in designing DSB-SC modulating circuit

Name of the subcircuit	Components used	Resultant frequency
Oscillator 1 (message signal generator) [Fig.4.2]	R=911Ω, C=12.1nF,C_f=0.9nF	25KHz
Oscillator 2 (carrier signal generator) [Fig.4.2]	R=207.6Ω, C=12.1nF, C_f=0.9nF	110KHz
Multiplier [Fig. 5, Ref. No. 42]	V_C=2V, V_{C1}=1V, V_{C2}=1.25V	---

5.1.1.2 Simulation Result

To simulate the circuit of Fig.5.3 on Pspice, ±1.5V supply voltages and 25μA biasing current and TSMC 180nm parameter files have been taken. Results are shown below:

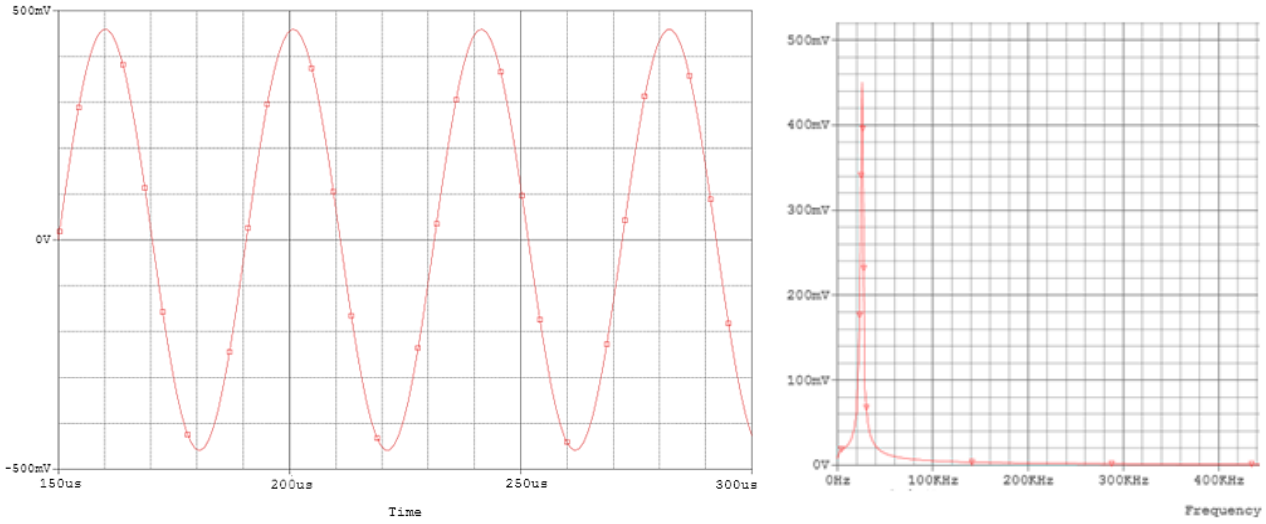

(i) (ii)

Fig. 5.4 Output of oscillator 1: (i)Message signal m(t), (ii) FFT of m(t)

From the frequency spectrum of Fig. 5.4(ii) we can see that the frequency of messagae signal is 24.6KHz

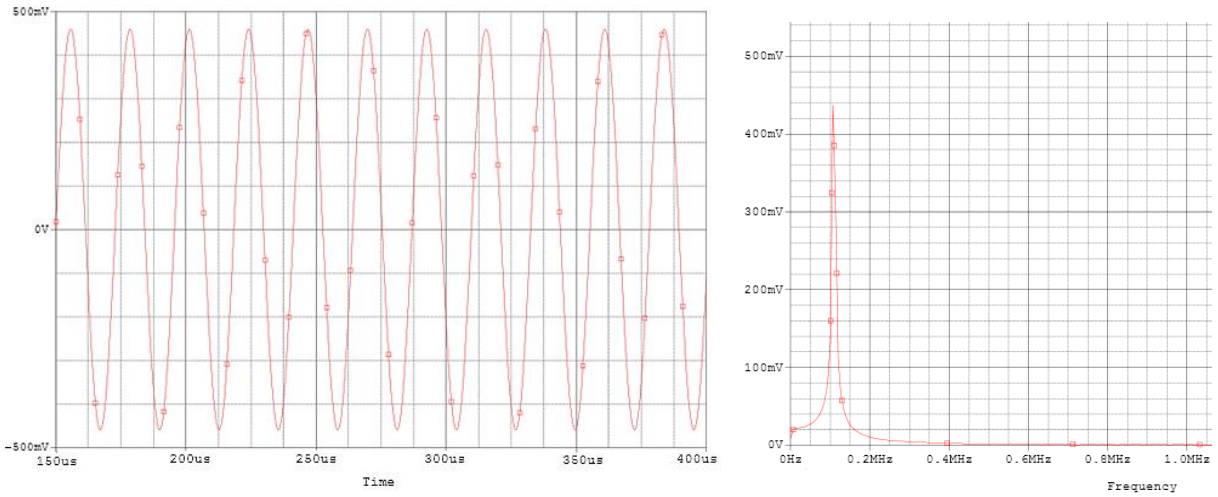

(i) (ii)

Fig. 5.5 Outputs of oscillator 2: (i) carrier signal (ii) its FFT

Thus from Fig.5.5(ii), frequency of carrier signal is found to be 109.5KHz which is slightly deviated from its theoretical value.

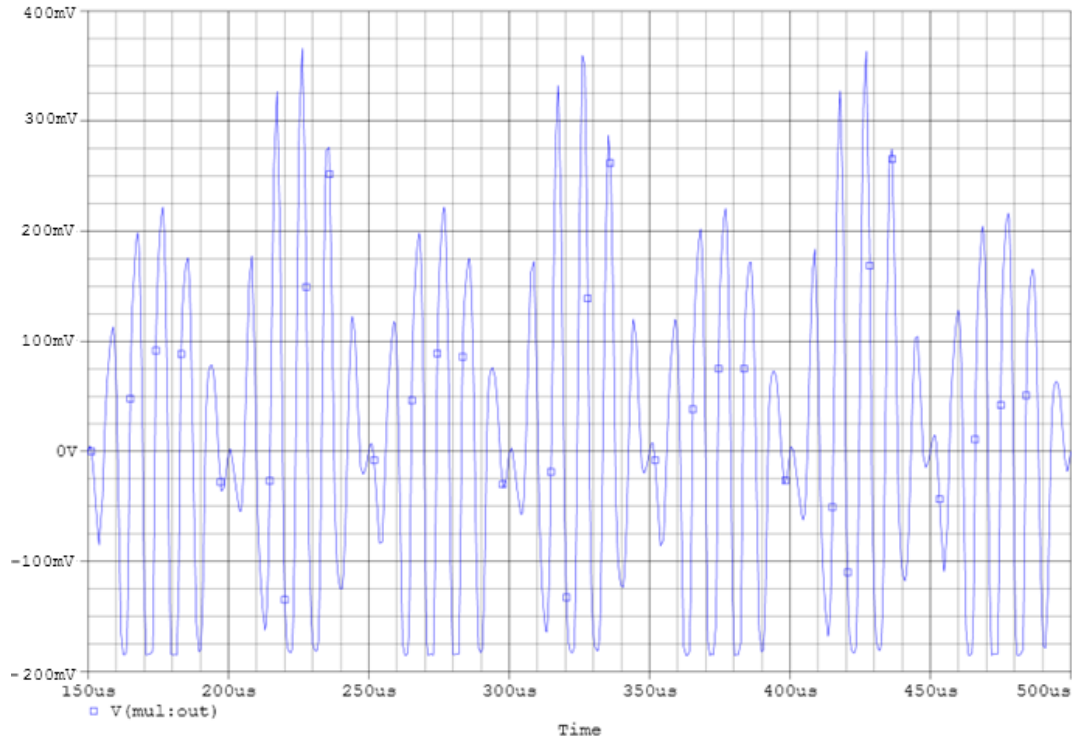

Fig. 5.6 DSBSC modulated output

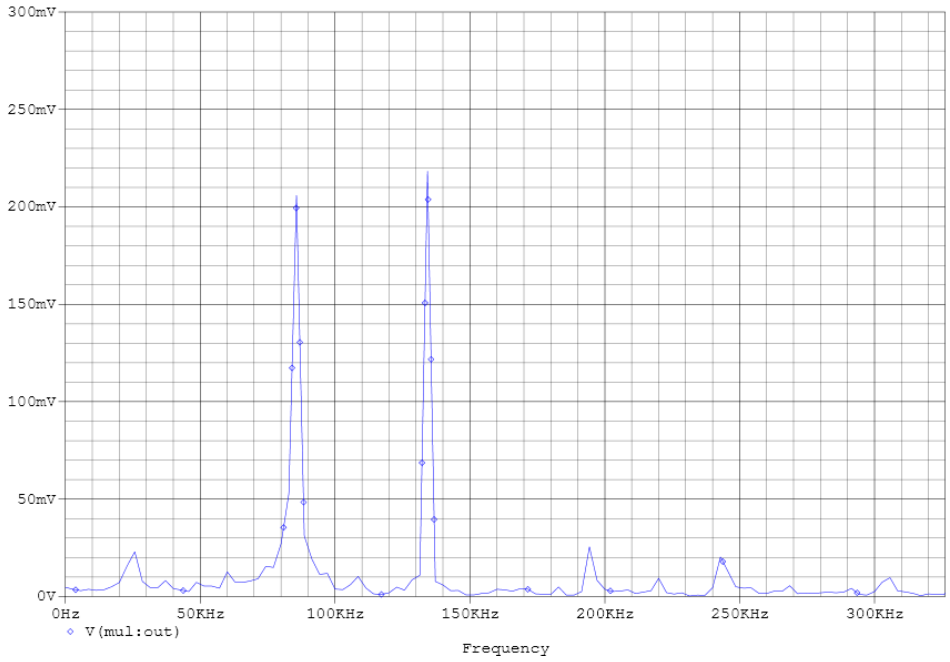

Fig. 5.7 frequency spectrum of modulated signal

Fig. 5.6 & 5.7 present modulated output. According to theory we should get two impulses at 85KHz & 135KHz after modulation. From Fig. 5.7 we can see that the resultant frequency spectrums are present at 84KHz & 133KHz. A table containing all the details of simulation results and experimental values has been given in the next page.

Table 5.2 Result analysis

	Parameters	Theoretical values	Experimental results
1.	Message signal frequency, f_m	25KHz	24.6KHz
2.	Carrier signal frequency, f_c	110KHz	109.5Hz
3.	Frequency spectrum of USB of modulated signal	135KHz	133KHz
4.	Frequency spectrum of LSB of modulated signal	85KHz	84KHz
5.	Bandwidth	50KHz	49KHz
5.	Deviation in USB of modulated signal	---	1.4%
6.	Deviation in LSB of modulated signal	---	1.7%

As there are very less deviation of below 2%, the circuit of Fig.5.3 is proved to be an excellent analog modulator.

5.1.2 DSB-SC DEMODULATION

The process of extracting the original message signal from modulated signal is known as 'demodulation' or 'detection'[46]. In the case of DSB signals, synchronous or coherent detection is used. Here, the same carrier frequency that was used in modulation needs to be generated by the LO. Fig. 5.8 shows the block diagram of coherent detector. DSB-SC modulated signal is multiplied with a carrier of same frequency and then passed through LPF to extract the original message signal.

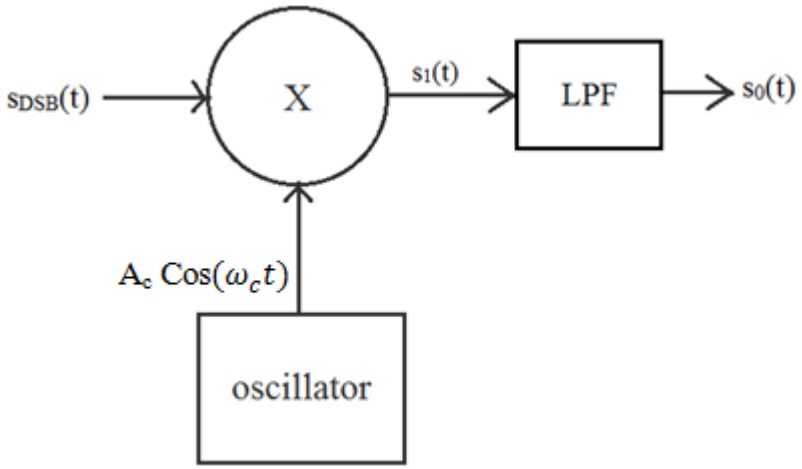

Fig. 5.8 Demodulation of DSBSC using synchronous detector

From equation (5.4) we have already got the input signal $S_{DSB}(t)$ that was the output of the transmitter. This signal will now be passed through a channel and then be received by the receiver and detection is done. Mathematically the whole process [46] can be expressed as,

$$S_1(t) = S_{DSB}(t)\, A_c Cos(\omega_c t) \tag{5.5}$$

From equation (5.4),

$S_{DSB}(t) = A_c m(t) Cos(\omega_c t)$, therefore $S_1(t)$ can be expressed as

$$S_1(t) = [A_c m(t) Cos(w_c t)] A_c Cos(\omega_c t)$$

$$= A_C^2 m(t) Cos^2(\omega_c t)$$

$$= A_C^2 m(t)\left[\frac{1+Cos(2\omega_c t)}{2}\right]$$

$$= \frac{A_C^2 m(t)}{2} + \frac{A_C^2 m(t) Cos(2\omega_c t)}{2}$$

After passing through the LPF only first element of the above equation will remain, so final output $S_0(t)$ can be given as,

$$S_0(t) = \frac{A_C^2 m(t)}{2} \tag{5.6}$$

If the carrier frequency generated by LO is non-ideal and has a phase of $\emptyset$, then it will reflect at the output also and final output will be,

$$S_0(t) = \frac{A_C^2 m(t)}{2} Cos\emptyset$$

Since maximum and minimum values of $Cos\emptyset$ lie between ±1, it does not harm the output as long as it is not zero, i.e. $\emptyset$=90°. When $\emptyset$=90°, the output becomes zero which is called 'quadrature null effect'. This happens when we use two different carriers with 90° phase difference like one is sin and another cos, to the modulator and demodulator.

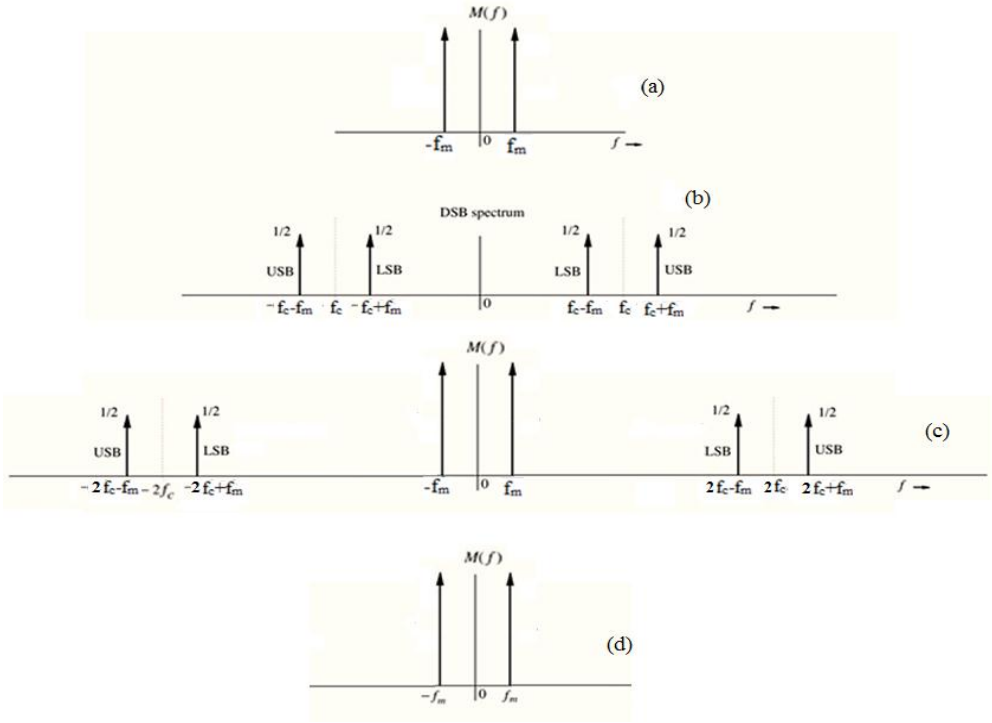

Fig. 5.9 Frequency spectrums of DSBSC (a)message signal (b)modulated signal (c) demodulated output (d)output of LPF

5.1.2.1Demodulation Of DSB-SC Signal Using OTRA Based Circuits

To demodulate DSB-SC signal, we need one oscillator, multiplier and one LPF. Former two were discussed in the previous section. One OTRA based LPF[43] is implemented with a cut-off frequency of 33KHz. Cut-off frequency is taken slightly greater than the frequency of message signal(25KHz) so that no loss incurred. Fig. 5.10 portrays circuit diagram of OTRA based coherent detector and Table 5.3 represents values of different components used while designing it.

Table 5.3: Component values taken to design the coherent detector

Name of the subcircuit	Components used	Resultant frequency
Oscillator 2 (carrier)	R=207.6Ω, C=12.1nF, C_f=0.6nF	f_c=110KHz
Multiplier [Fig.5, Ref. No.-42]	V_C=2V, V_{C1}=1V, V_{C2}=1.25V	---
LPF [Fig.3 of Ref. No.-43]	R_{a1}=205KΩ, R_{a2}=25KΩ, R_b=100KΩ, R_c=200KΩ, R_d=200KΩ, C_a=120nF, C_b=1pF , C_c=1nF, C_d =5pF	Cut off frequency, f_0=32KHz

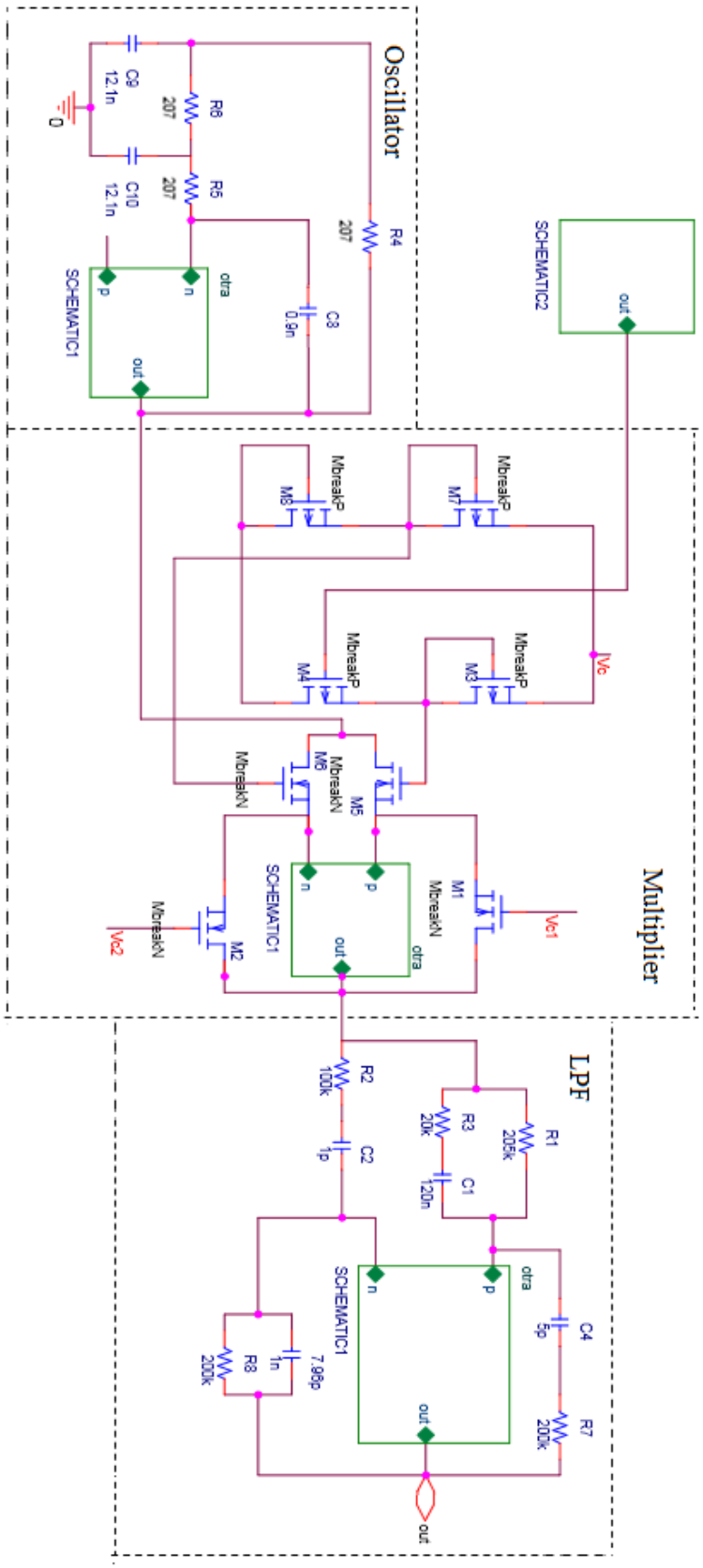

Fig.5.10 OTRA based Coherent detector

5.1.2.1 Simulation Result

The OTRA based coherent detector shown in Fig.5.10 is simulated on PSPICE simulator using the TSMC 180nm process parameters and ±1.5V of supply voltages. Biasing current remains same as it was(25µA). The generated DSB-SC signal from the previous section has been used as the message signal to the demodulator. Results are depicted below:

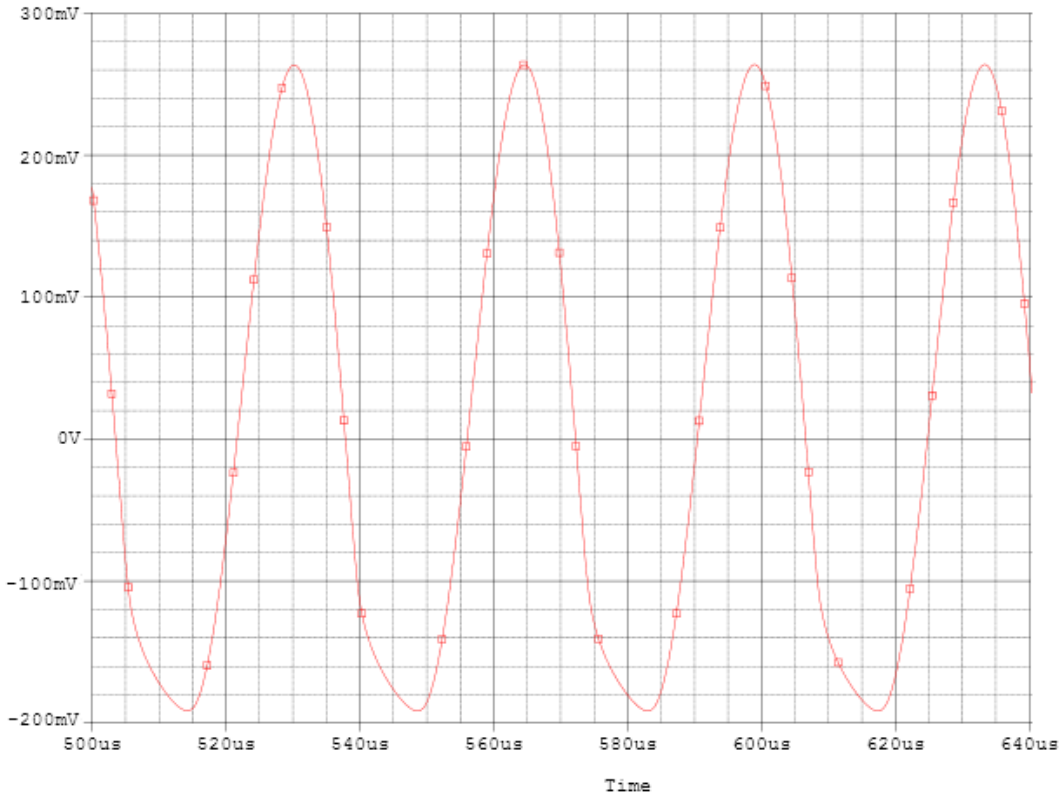

Fig. 5.11 Demodulated output

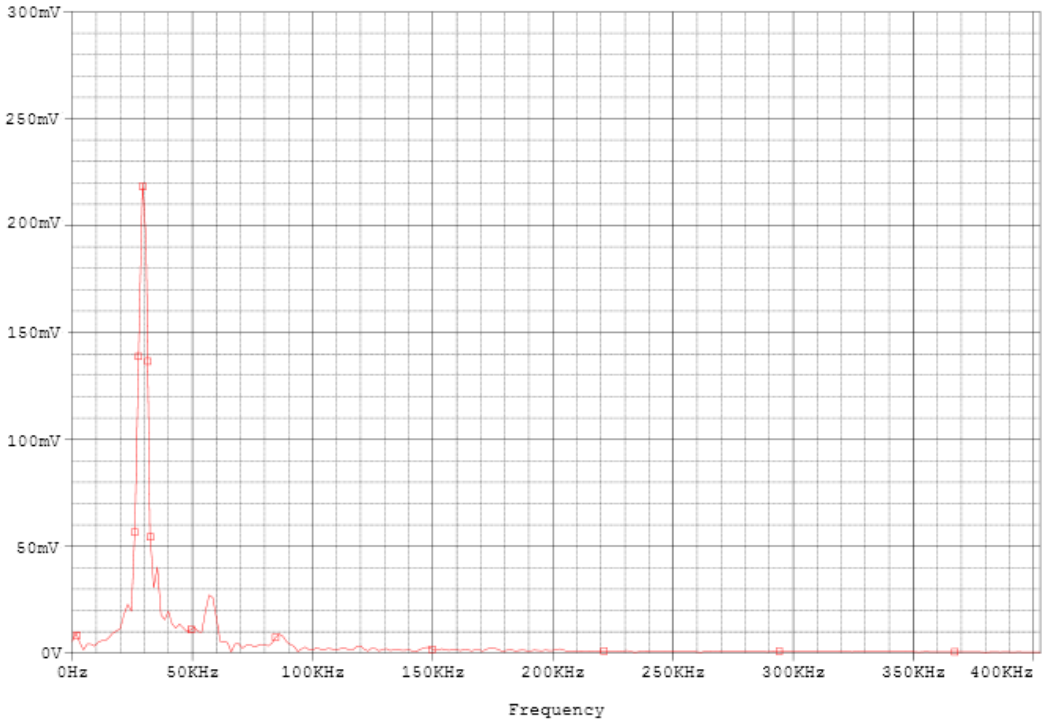

Fig. 5.12 FFT of Demodulated signal

Fig. 5.11 and 5.12 show the demodulated output after passing through LPF. Theoretically the frequency spectrum of demodulated signal should be present at 24.6KHz and from Fig. 5.12 we can see the spike of the signal at 23.8KHz. There is a slight deviation in its spectrum which is less that 4% and is therefore acceptable. Whole analysis has been presented in Table 5.4.

Table 5.4 Result analysis

Parameters	Theoretical values	Experimental results
Frequency of modulated signal(before demodulation) [data from Table 5.2]	25KHz	24.6Hz
Frequency spectrum of demodulated output	24.6KHz	23.8KHz
Deviation in frequency		3.2%
Bandwidth of modulated signal(before demodulation) [data from Table 5.2]	50KHz	49KHz
Bandwidth of demodulated signal	49KHz	47.6KHz
Deviation in bandwidth		2.8%

So from Table5.4 clearly shows that there is a slight deviation in bandwidth of message signal and demodulated signal. Frequency spectrum is also slightly deviated from its original place. But these deviations are as less as 3-4%.

5.1.3 DSB-FC MODULATION

The term 'amplitude modulation' essentially refers to Double Side Band Large Carrier (DSBLC) or Double Side Band Full Carrier Modulation[46] because carrier is present in the modulated signal. It is used mainly for broadcasting in radio transmitter and picture transmission in a TV system. Due to presence of carrier signal power requirements increases in transmission of DSBFC.

There are various methods available for producing an AM signal. Particularly for DSBFC, Square law modulator(SLM) and switching modulator are popular. In this section generation of DSBFC using SLM will be discussed and realised with the help of OTRA based circuits.

Assume message signal, $m(t) = A_m Cos(\omega_m t)$

And carrier signal, $c(t) = A_c Cos(\omega_c t)$

Modulated wave,

$$S(t) = A_c Cos(\omega_c t) + [A_c Cos(\omega_c t)][A_m Cos(\omega_m t)] \quad (5.7)$$

$$= A_c[1 + \mu Cos(\omega_m t)]Cos(\omega_c t) \quad (5.8)$$

Where, $\mu = \frac{A_m}{A_c}$ (5.9)

Where, A_m is the amplitude of the message signal and A_c is the amplitude of the carrier signal. So to $\mu = 1$,

$$A_m = A_c \quad (5.10)$$

Amplitude modulation index(μ) is an important factor in the case of DSBFC signal since it is a measure of extent of amplitude variation about an unmodulated carrier. It indicates percentage of modulation and determines recovery of message from the modulated signal. In the case of AM, when μ exceeds unity distortion happens and from the modulated output message signal cannot be recovered properly. We get hundred percent modulation when modulation index equals unity. Fig. 5.13 & 5.14 exhibit DSB–FC Modulation and its generation using SLM.

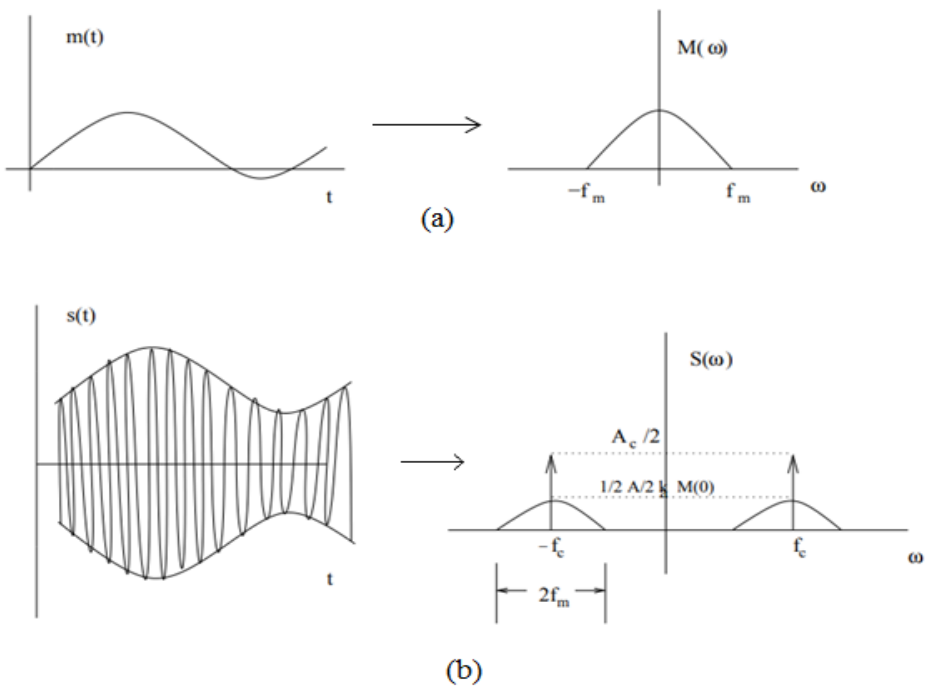

Fig. 5.13 DSB–FC Modulation: (a) message signal (b) modulated signal

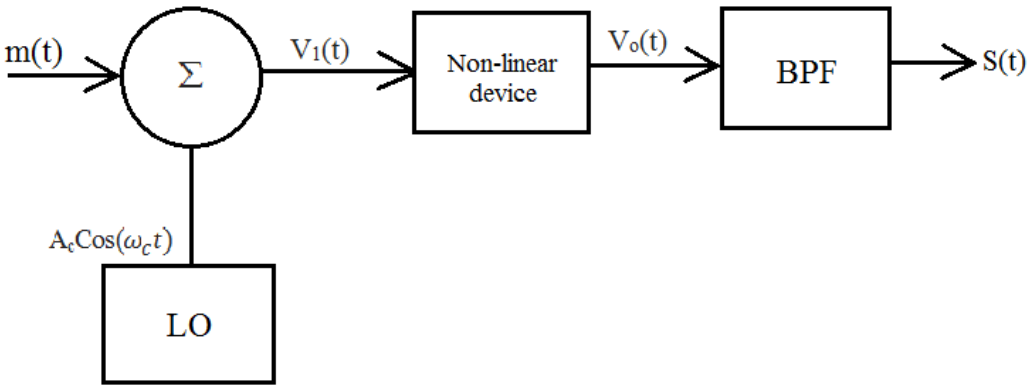

Fig. 5.14 Generation of DSBFC using SLM

Nonlinear device is used to multiply the signal with itself. Band pass filter(BPF) is used to select signal having proper band of frequency from the output wavefrom of nonlinear device and produces that as the final output. Mathematical expressions are given below:

$$V_0(t) = a_1 V_1(t) + a_2\big(V_1(t)\big)^2 + a_3\big(V_1(t)\big)^3 \quad (5.11)$$

$$V_1(t) = m(t) + A_c Cos(w_c t) \quad (5.12)$$

$$V_0(t) = a_1[m(t) + A_c Cos(w_c t)] + a_2[m(t) + A_c Cos(w_c t)]^2 + a_3[m(t) + A_c Cos(w_c t)]^3 \quad (5.13)$$

$$= a_1[m(t) + A_c Cos(w_c t)] + a_2[m^2(t) + 2m(t)A_c Cos(w_c t) + A_C^2 Cos^2(w_c t)] + a_3[m^3(t) + 3m^2(t)A_c Cos(w_c t) + 3m(t)A_c Cos^2(w_c t) + A_c^3 Cos^3(w_c t)] \quad (5.14)$$

Neglecting all the square and cube terms and passing through the band pass filter with centre frequency f_c and bandwidth equals message signal bandwidth ($2f_m$) we get,

$$S(t) = a_1 A_c Cos(w_c t) + 2a_2 m(t) Cos(w_c t) \quad (5.15)$$

$$= a_1 A_c \left[1 + \frac{2a_2}{a_1}\right] Cos(w_c t) \quad (5.16)$$

Thus we get amplitude modulation index,μ equals $\frac{2a2}{a1}$, while using a square law modulator.

5.1.3.1 Generation of DSB-FC Signal Using OTRA Based Circuits

Amplitude modulation is possible using OTRA based circuits. To do this every block of Fig. 5.14 is replaced by their OTRA based counterparts. To generate message signal and carrier signal, oscillator[section 4.2] is used with different resonant frequencies. Multiplier that was used also in DSBSC is used here as a squarer[42]. And one universal filter reported in [43] is used to work as a BPF with centre frequency of 225KHz. Fig. 5.15 shows the circuit diagram of OTRA based DSBFC Generator.

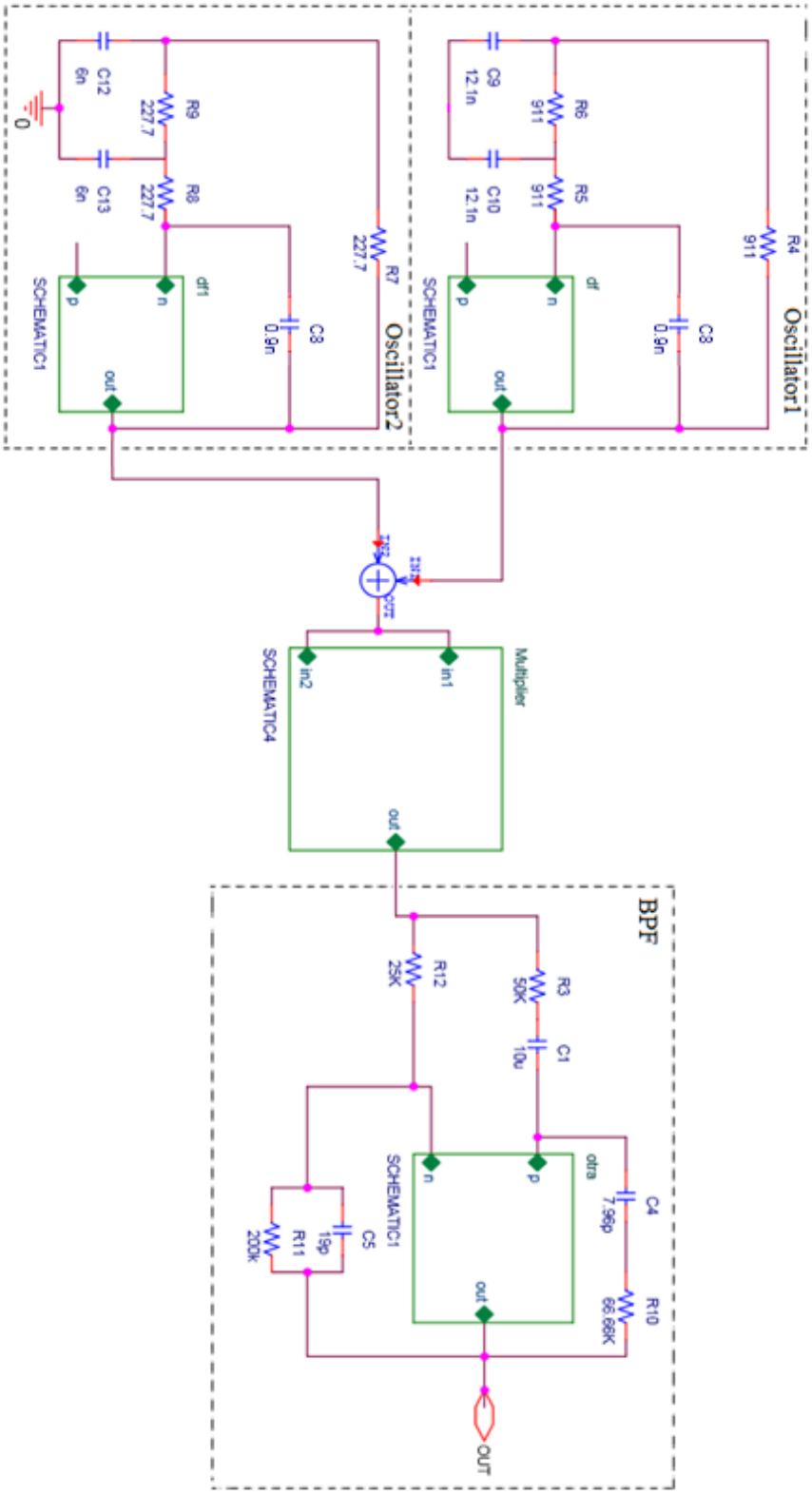

Fig. 5.15 Circuit diagram of DSBFC Generator

Table 5.5 Component values of OTRA based DSBFC Generator

Name of the subcircuit	Components used	Resultant frequency
Oscillator 1 [Fig.4.2]	R=911Ω, C=12.1nF, C_f=0.9nF	25KHz
Oscillator 2 [Fig.4.2]	R=156.6Ω, C=8nF, C_f=0.9nF	220KHz
Multiplier [Fig.5, Ref. No.- 42]	V_C=2V, V_{C1}=1V, V_{C2}=1.25V	---
BPF [Fig.3, Ref. No.- 43]	R_a=50KΩ, R_b=100KΩ, R_c=200KΩ, R_d=66.6KΩ, C_a=7.96pF=C_b, C_c=1nF, C_d =5.97pF	centre frequency=220KHz

5.1.3.2 Simulation Results

The circuit of Fig.5.15 is simulated on PSPICE using the TSMC 180nm process parameters with supply voltages of ±1.5V and 25µA biasing current. The resultant graphs have been shown below:

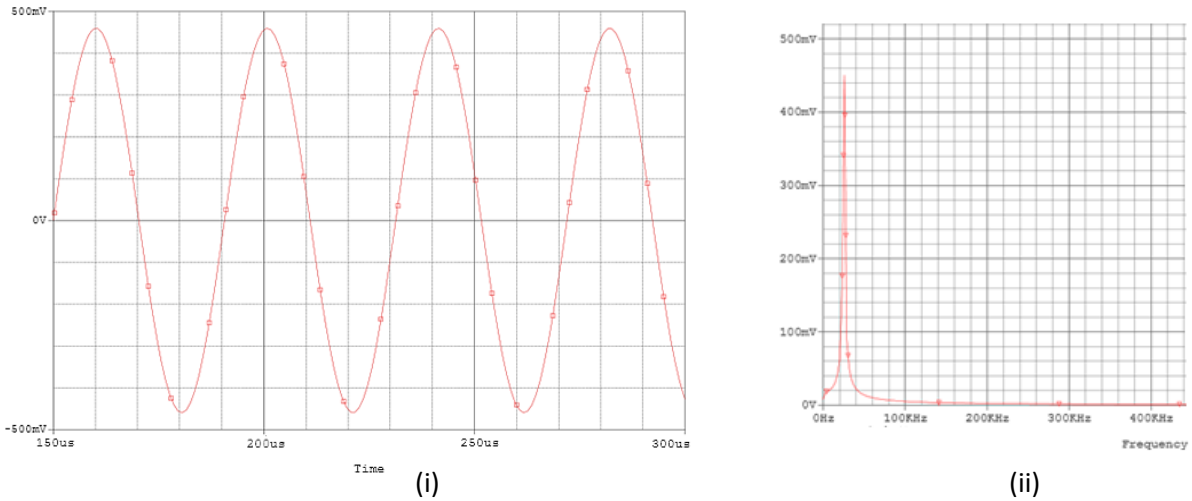

(i) (ii)

Fig.5.16 output of oscillator1: (i) message signal (ii)FFT of message signal

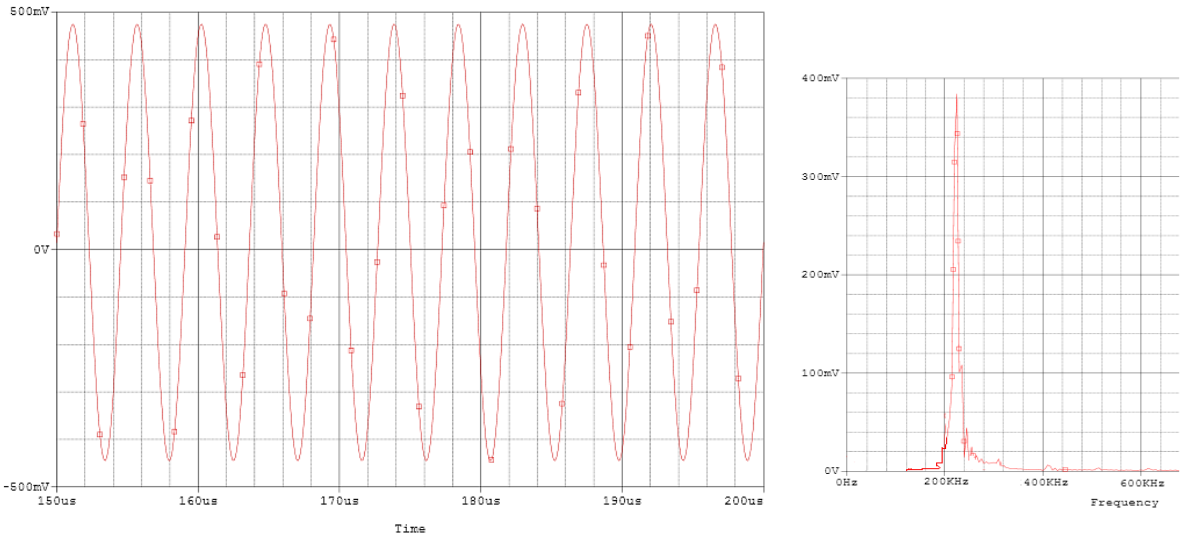

(i) (ii)

Fig.5.17 Output of oscillator2: (i)carrier signal (ii)FFT of carrier signal

Fig. 5.16 & 5.17 present message and carrier signals respectively. From the frequency spectrums shown in 5.16(ii) & 5.17(ii), we can see that the signals are present at 24.6KHz & at 221.3KHz.

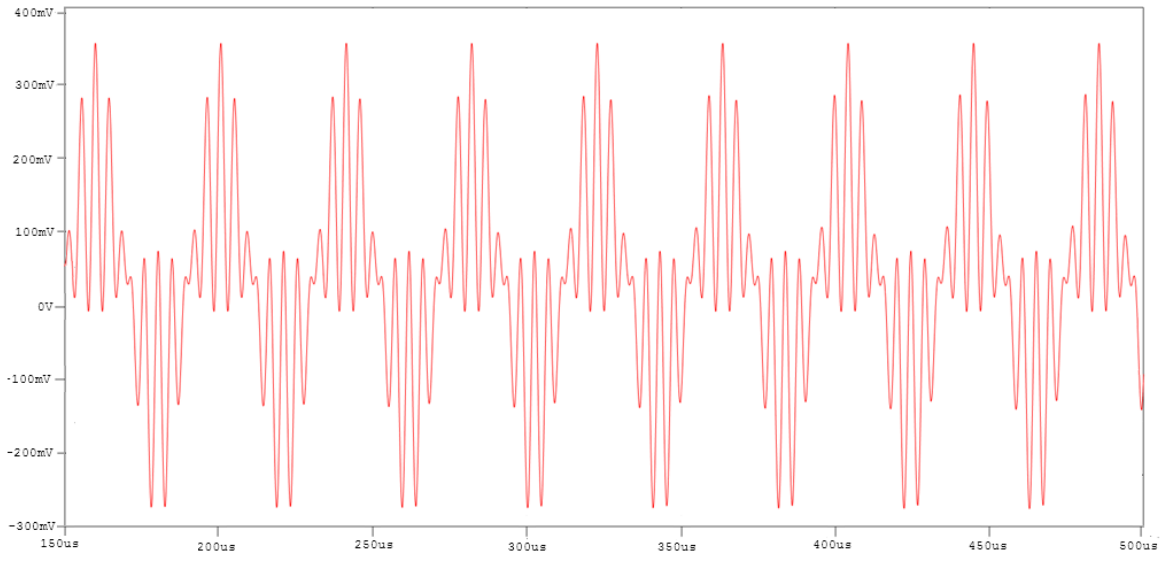

Fig.5.18 DSBFC modulated output when μ=1

Fig. 5.18 shows DSBFC modulated output when modulation index(μ) is 1. It happens when amplitude of message signal and carrier signal are equal(equation 5.9).

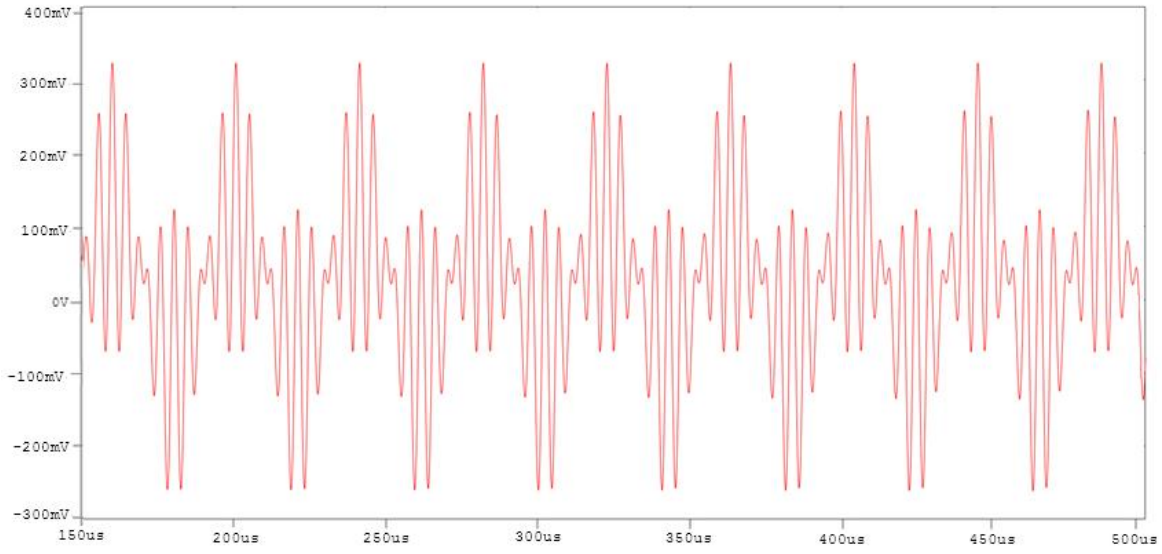

Fig.5.19 DSBFC modulated output when μ=1.5

The above graph is plotted when depth of modulation is 1.5 i.e. that ratio between the amplitude of message signal and the amplitude of carrier signal is 1.5. As value of μ increases, percentage of modulation is also increased and message signal cannot be recovered back at the demodulator. From the Fig. 5.19 we can see that the signal is failed to follow a perfect 0V axis. As it is a distorted signal, it cannot be properly demodulated by the demodulator and we fail to extract the original message signal from the modulated output. The output waveform is drawn only to show DSBFC modulation for μ≥1.

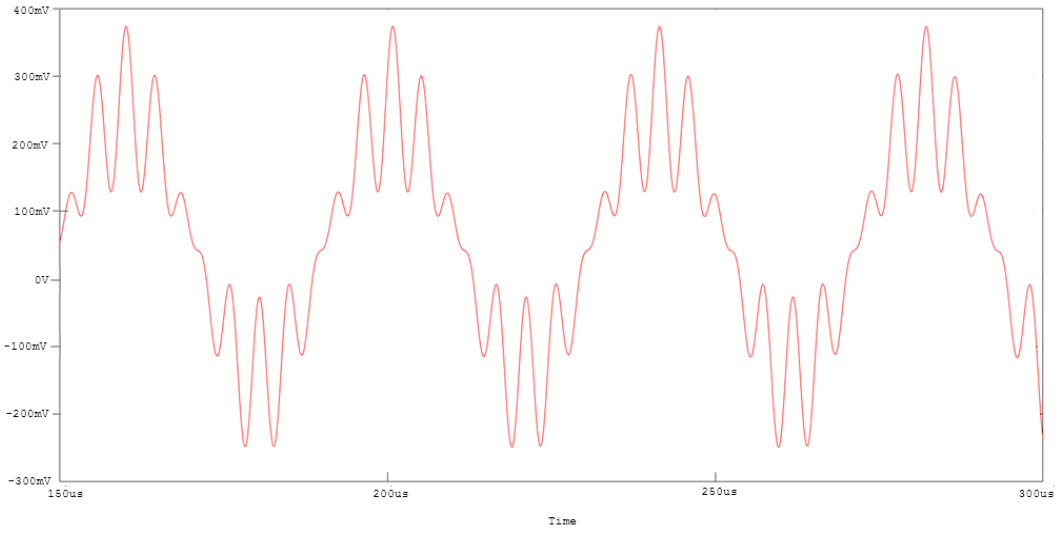

Fig.5.20 DSBFC modulated output when μ=0.6

The above figure shows modulatated output when μ is less than 1. Undistorted modulation is happened here and we can easily recover the original message signal from this modulated waveform.

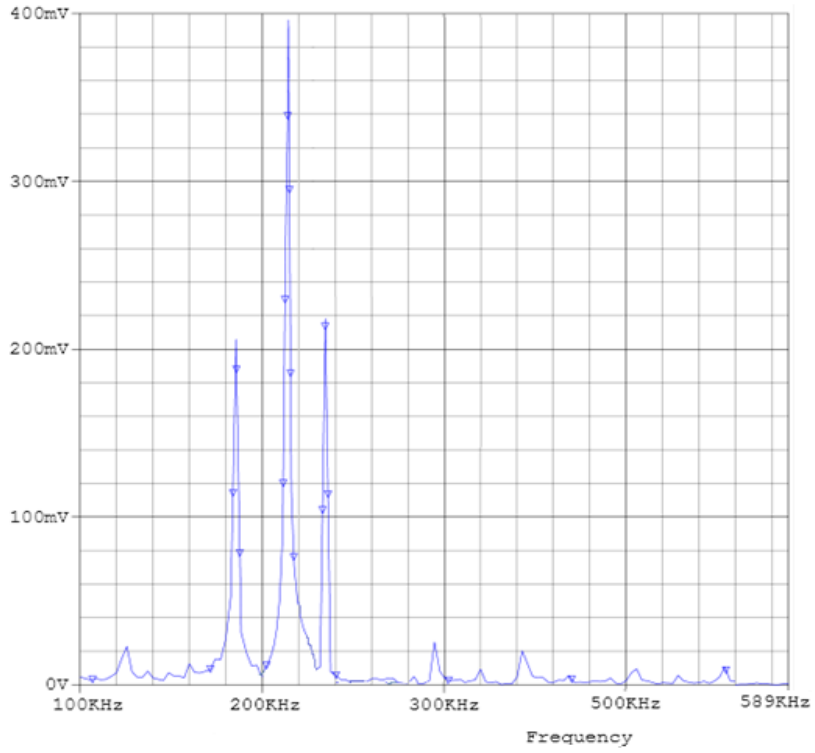

Fig.5.21 Frequency spectrum of DSBFC modulated output

Frequency of the signal does not depend on the value of modulation index,μ. It depends only on the resonant frequencies of message and carrier signals. Theoritically, frequency spectrum of modulated signal should be present at 185KHz & 235KHz and experimental values are 186KHz & 236.5KHz. Analysis has been done in Table 5.6

Table 5.6 Result Analysis with μ=1, supply voltages=±1.5V

	Parameters	Theoretical values	Experimental results
1.	Message signal frequency, f_m	25KHz	24.6KHz
2.	Carrier signal frequency, f_c	220KHz	221.3KHz
3.	Frequency spectrum of USB of modulated signal	235KHz	236.5KHz
4.	Frequency spectrum of LSB of modulated signal	185KHz	186KHz
5.	Bandwidth	50KHz	50.5KHz
6.	Changes in Bandwidth	---	1%

As there are very low distortion of BW(1%), this DSBFC modulator(Fig.5.15) is proved to be an excellent modulator and can be used in communication systems.

AM transmitters and receivers are simple and cost effective, since no specialized components are needed. AM waves can travel a longer distance, therefore in commercial broadcasting they are used. But to send and receive two sidebands bandwidth requrements is more in DSBSC & DSBFC. Another disadvantage is wastage of power in the case of DSBFC signal. For 100% modulation, the maximum power carried by AM waves is only 33.33%. Efficiency decreases with the decrease in modulation index. And since they are amplitude dependent, so more noise prone.

5.2 PAM

In pulse amplitude modulation(PAM), the signal is sampled at regular intervals and each sample is made proportional to the amplitude of the modulating signal[44]. A periodic pulse train is used as a carrier. The pulse may take any real voltage value that is proportional to the value of the original waveform. Pulses can be of a rectangular form or any other appropriate form. During this process no information is lost, but the energy is redistributed in the frequency domain. Power varies due to change in amplitude of the pulses. PAM is similar to natural sampling with a slight difference. Both in natural sampling and PAM the message signal is multiplied by a periodic train of pulses but in the former process the top of each modulated rectangular pulse varies in accordance with the message signal whereas in the latter one remains flat. So PAM resembles more with flat-top sampling than natural sampling. In this chapter generation of PAM signal is described briefly and then its OTRA implementation is done.

In this section generation of PAM signal is discussed and then it is realized using OTRA based circuits. Fig.5.22 shows pictorial representation of pulse amplitude modulation.

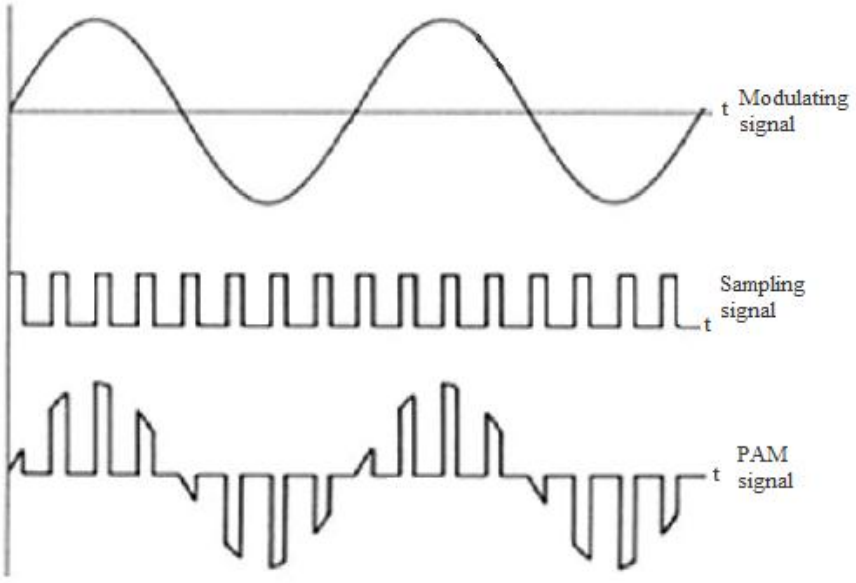

Fig. 5.22 PAM signal

Let S(t) denote the sequence of flat-top pulses generated as shown in the Fig. 5.22.

Mathematically S(t) can be represented[44] as,

$$s(t) = \sum_{n=-\infty} m(nT_s)h(t - nT_s) \tag{5.17}$$

Where h(t) is a rectangular pulse of time period T and unit amplitude. Let h(T_s) be sampled version of h(t). Mathematically h(t) can be written as,

$$h(t) = \begin{cases} = 1, & 0 \le t \le T \\ = \frac{1}{2}, & t = 0, t = T \\ = 0, & otherwise \end{cases} \tag{5.18}$$

The instantaneously sampled version of message signal m(t) is given by,

$$m_\delta(t) = \sum_{n=-\infty}^{\infty} m(nT_s)\delta(t - nT_s) \tag{5.19}$$

From equation (5.2.1) & (5.2.3) we get,

$$m_\delta(t) * h(t) = \int_{-\infty}^{\infty} m_\delta(\tau)h(t - \tau)d\tau$$

$$= \int_{-\infty}^{+\infty} \sum_{n=-\infty}^{+\infty} m(nT_s)\delta(\tau - nT_s)h(t - \tau)d\tau$$

$$= \sum_{n=-\infty}^{+\infty} m(nT_s) \int_{-\infty}^{+\infty} \delta(\tau - nT_s)h(t - \tau)d\tau \tag{5.20}$$

Using shifting property of delta function,

$$s(t) = m_\delta(t) * h(t) = \sum_{n=-\infty} m(nT_s)h(t - nT_s) \tag{5.21}$$

In frequency domain equation (5.2.5) can be written as,

$$S(\omega) = M_{\delta}(\omega) * H(\omega)$$

$$= \frac{\omega_S}{2\pi} \sum_{K=-\infty}^{\infty} M(\omega - k\omega_s) H(\omega) \tag{5.22}$$

Fig. 5.23 shows the process of generating PAM signal. It has a very simple circuitry with only one multiplier and one oscillator and train of pulses. To make train of pulses one OTRA based square wave generator [41] is used. This square wave generator uses only one OTRA, two resistors and one capacitor. It is electronically tunable and its duty cycle can be adjusted with the help of passive elements and input voltage.

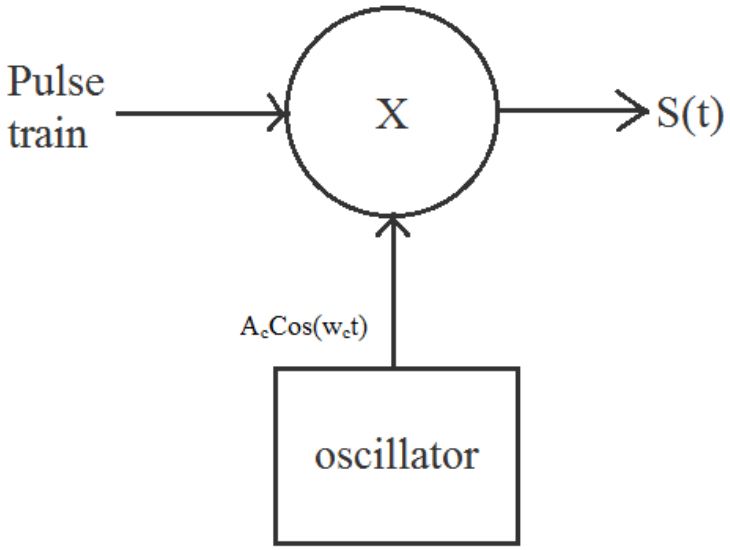

Fig. 5.23 Generation of PAM Signal

5.2.1 REALIZATION OF PAM USING OTRA

To generate PAM signal, each subpart of the circuit of Fig.5.23 has been implemented individually and then cascaded properly. One OTRA based square wave generator reported in [41] is used to produce train of pulses that will be given as an input to the multiplier. The generator is electronically tunable through the passive elements (R & C) used there.

Table 5.6 Component values used in designing of PAM generator

Name of the subcircuit	Components used	Resultant frequency
Square wave generator [Fig.3(b), Ref. No.-41]	R1=2KΩ, R2=1.97KΩ, C=220nF	47KHz
Oscillator 2 [Fig.4.2]	R=207.6Ω, C=12.1nF, C_f=0.9nF	110KHz
Multiplier [Fig.5, Ref. No.42]	V_C=2V, V_{C1}=1V, V_{C2}=1.25V	---

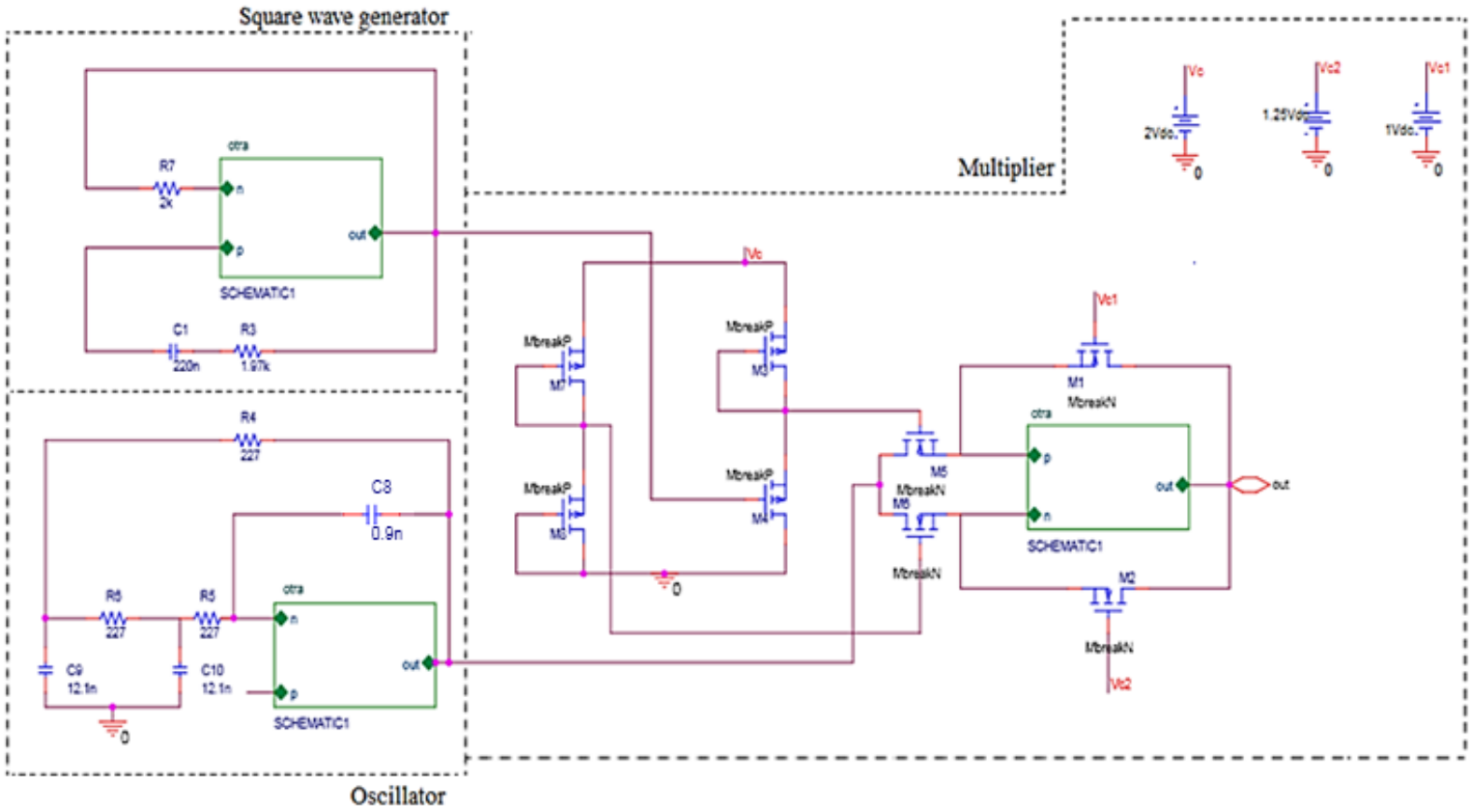

Fig. 5.24 Circuit Diagram of generation of PAM

5.2.2 SIMULATION RESULT

Fig. 5.2.3 shows the experimental result of square wave generator[40]. Fast Fourier analysis of train of pulses has been done and shown in Fig. 5.2.4. And generated PAM signal is given in Fig. 5.2.5

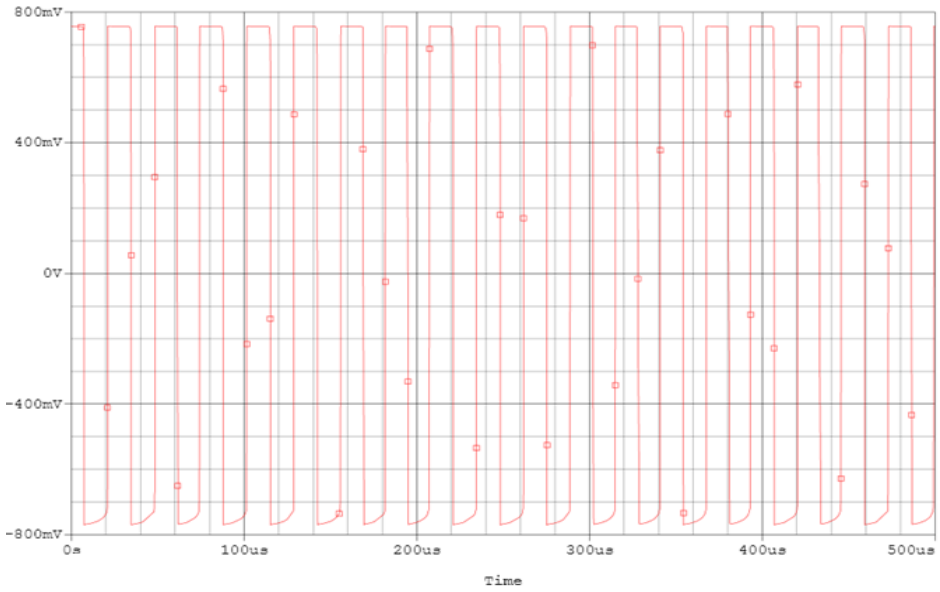

Fig. 5.25 Output of square wave generator - pulse train

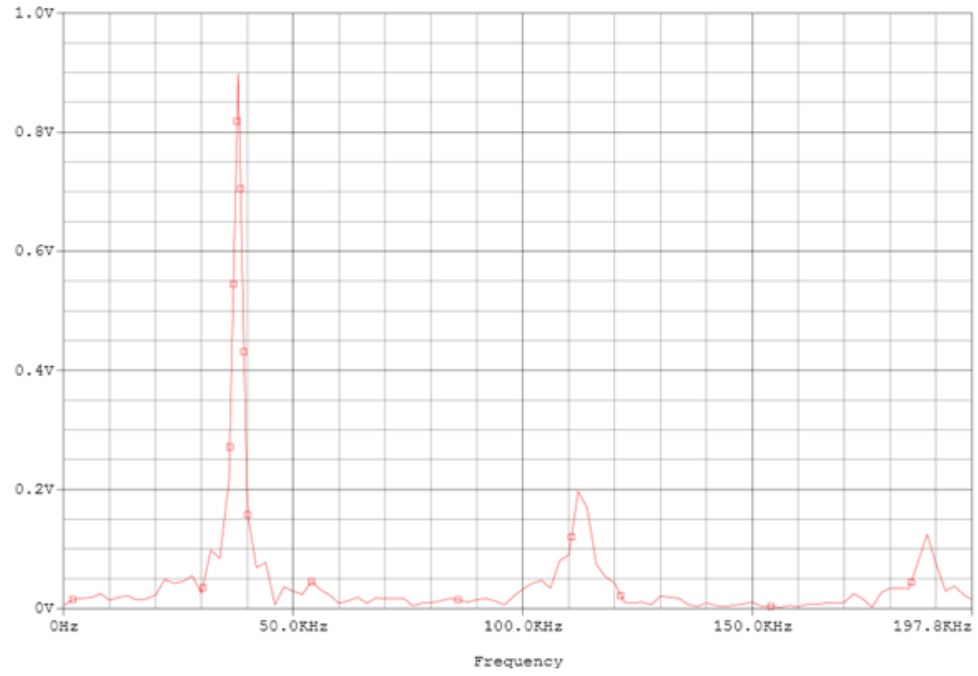

Fig. 5.26 FFT of pulse train

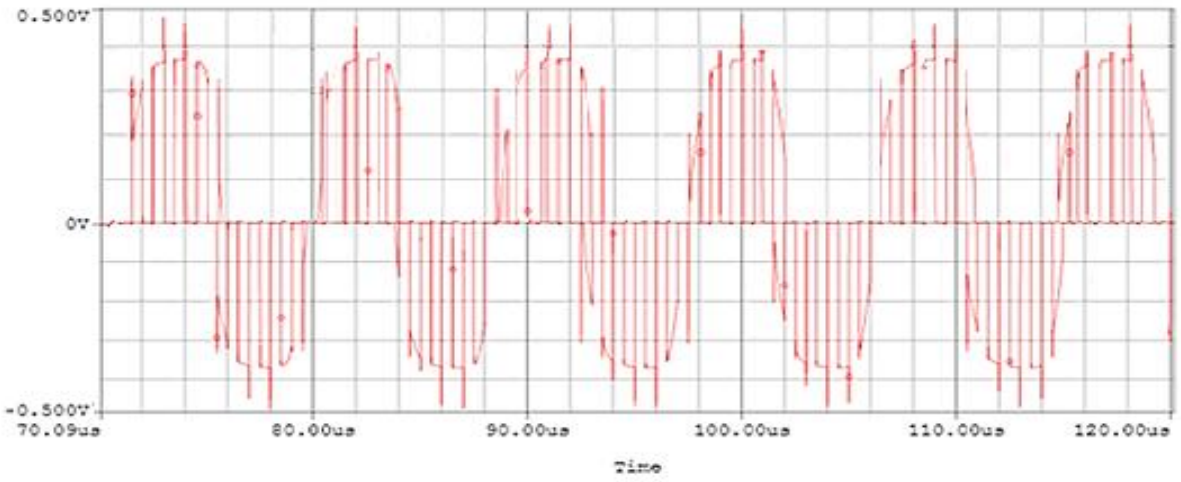

Fig. 5.27 Generated PAM signal

This is a double polarity PAM where we get both positive and negative pulses in the output. In the case of single polarity PAM, fixed DC bias is added to ensure all the pulses positive. PAM is widely used[47] in establishing Ethernet network like LAN, WLAN etc. PAM generates control signals in microcontrollers, electronic LED drivers, photo-biology devices and used extensively.

CHAPTER 6

CONCLUSIONS AND SCOPE FOR FUTURE WORK

6.1 CONCLUSIONS

Study and analysis of OTRA has been done. One CMOS based OTRA is implemented using Pspice. This OTRA has been taken into account for evaluation of OTRA based circuits like sinusoidal oscillator, LP & BP filters, square wave generator and integrator. All of the mentioned circuits are important building blocks while making any communication module. Different modulation schemes like DSB-SC, DSB-FC, PAM are implemented and verified through Pspice. DSB-SC demodulation is also done and which is matched to the message signal ignoring less distortions. A quadrature oscillator is designed with the help of the CMOS based OTRA and integrator. Frequency spectrums are plotted for verification.

6.2 SCOPE FOR FUTURE WORK

Other communication schemes like frequency & phase modulation & demodulation, ASK, PSK, FSK etc can be realized with the help of only OTRA based circuits like oscillator, integrator, filters etc. To decrease the supply voltage and power consumption, OTRA can be implemented in the submicro-volt region and MOS-C implementation can be done to lower the chip area.

REFERENCE

1. Wilson, B. Recent developments in current conveyors and current-mode circuits. IEE Proc. G Circuits Devices Syst. 1990, 137, 63–77.
2. Schmid, H. " Why "current mode" does not guarantee good performance", Analog Integr. Circuits Signal Process. 2003, 35, 79–90.
3. J. J. Chen, H. W. Tsao, C. C. Chen, "Operational transresistance amplifier using CMOS technology" Electronics Letters, vol. 28, pp. 2087–2088, 1992.
4. K. N. Salama, A. M. Soliman, "CMOS operational transresistance amplifier for analog signal processing applications," Microelectronics Journal, vol. 30, pp. 235–245, 1999.
5. H. O. Elwan, A. M. Soliman, "CMOS Differential Current Conveyors and applications for analog VLSI," Analog Integrated Circuits and Signal Processing, vol. 11, pp. 35–45, 1996.
6. A. Ravindran, A. Salva, I. Younus, M. Ismail, " A 0.8V CMOS filter based on a novel low voltage operational transresistance amplifier," Proc. IEEE Midwest Symposium on Circuits and Systems, pp. III 368–III 371, 2002.
7. A. Rahman, K. Kafrawy, A. M. Soliman,"A modified CMOS differential operational transresistance Amplifier(OTRA)," International Journal of Electronics and Communication (AEU), vol. 63, pp. 1067–1071, 2009.
8. C. L. Hou, H. C. Chien, Y. K. Lo, " Square wave generators employing OTRAs," IEE Proceedings Circuits Devices and Systems, vol.152, pp. 718–722, 2005.
9. C. Sanchez-Lopez, E. Martinez-Romero, E. Tlelo-Cuautle, " Symbolic Analysis of OTRAs- Based Circuits," Journal of Applied Research and Technology, vol. 9, pp. 69–80, 2011.
10. Salama, K. N. and Soliman, A. M., "Novel Oscillators Using the Operational Transresistance Amplifier," Microelectron. J., Vol. 31, No. 1, pp. 3947 (2000)
11. U. Cam, "A Novel Single- Resistance- Controlled Sinusoidal Oscillator Employing Single Operational Transresistance Amplifier", Analog Integrated Circuits and Signal Processing, vol. 32, pp. 183–186, 2002.

12. Rajeshwari Pandey, Neeta Pandey, Sajal K. Paul "MOS-C Third Order Quadrature Oscillator using OTRA," Third International Conference on Communication and Computer Technology (ICCCT'12), pp.77 – 80, Nov. 2012.
13. Rajeshwari Pandey, Neeta Pandey, Mayank Bothra,and Sajal K. Paul "Operational Transresistance Amplifier-Based Multiphase Sinusoidal Oscillators," Journal of Electrical and Computer Engineering Volume 2011, Article ID 586853, 8 pages.
14. Pandey, R., Pandey, N., Mullick, R., Yadav, S., & Anurag, R. " All pass network based MSO using OTRA", Advances in Electronics, Hindawi Publishing Corporation, 2015, Article ID 382360, 1–7.
15. Nagar, B. C., & Paul, S. K. " Voltage mode third order quadrature oscillators using OTRAs", Analog Integrated Circuits and Signal Processing-2016, 88(3), 517–530.
16. Komanapalli, G., Pandey, N., & Pandey, R, " New realization of quadrature oscillator using OTRA", International Journal of Electrical and Computer Engineering (IJECE)-2017, 7(4), 1815–1823.
17. J. J. Chen, H. W. Tsao, S. I. Liu, " Voltage - mode MOSFET – C filters using operational transresistance amplifiers (OTRAs) with reduced parasitic capacitance effect," IEE Proceedings Circuits Devices and Systems, vol. 148, pp. 242–249, 2001.
18. W. Chiu, J. H. Tsay, S. I. Liu, H. W. Tsao, J. J. Chen, "Single capacitor MOSFET-C integrator using OTRA," Electronics Letters, vol. 31, pp. 1796–1797, 1995.
19. Cakir, C., Cam, U., & Cicekoglu, O.," Novel all pass filter configuration employing single OTRA", IEEE Transactions on Circuits and Systems-II, 52(3), 122–125, 2005.
20. S. Kilinc, U. Cam, " Cascadable all pass and notch filters employing single operational transresistance amplifier," Computers and Electrical Engineering, vol.31, pp. 391–401, 2005.
21. Salama, K. N., & Soliman, A. M, "Active RC filters using operational transresistance amplifiers", Journal of Circuits, Systems and Computers, 8(4), 507–516, 1998.

22. Cam, U., Cakir, C., & Cicekoglu, O., "Novel transimpedance type first-order all pass filter employing single OTRA", AEU-International Journal of Electronics and Communication, 58(4), 296–298, 2004.
23. Gokcen, A., & Cam, U., "MOS-C single amplifier biquads using the OTRA", AEU- International Journal of Electronics and Communications, 63(8), 660–664, 2009.
24. Gokcen, A., Kilinc, S., & Cam, U., " Fully-integrated universal biquads using operational transresistance amplifiers with MOS-C realization", Turkish Journal of Electrical Engineering and Computer Science, 19(3), 363–372, 2011.
25. Singh, R., Ranjan, A., Ghosh, M., & Paul, S. K., " Realization of fourth order multifunction filters using operational transresistance amplifier", Journal of Electronic Design Technology, 2(2), 1–7, 2012.
26. Anurag, R., Pandey, N., Chandra, R., & Pandey, R., " Voltage mode second order notch/all- pass filter realization using OTRA", I-Manager's Journal on Electronics Engineering, 6(2), 22–28, 2015.
27. Gokcen, A., & Cam, U., " A 5th order video band elliptic filter topology using OTRA based Fleischer Tow biquad with MOS-C realization", Natural and Engineering Sciences, 1(2), 44–52, 2016.
28. Chang, C. M., Lin, Y. T., Hsu, C. K., Hou, C. L., & Horng, J. W. " Generation of voltage-mode OTRA-based multifunction biquad filter", Recent Researches in Instrumentation, Measurement, Circuits and Systems, 21–27, 2011.
29. Senani, R., Singh, A. K., Gupta, A., & Bhaskar, D. R., " Simple simulated inductor, low-pass/band-pass filter and sinusoidal oscillator using OTRA", Circuits and Systems, 7(3), 83– 99, 2016.
30. Dabas, A., & Arora, N., " Tunable filters using operational transresistance amplifiers", International Journal of Electrical and Electronics Engineering (IJEEER), 4(4), 103–112, 2014.
31. Soliman, A. M., " History and progress of the Tow–Thomas biquadratic filter part II: OTRA, CCII, and DVCC realizations", Journal of Circuits, Systems and Computers, 17(5), 797–826, 2008.

32. Rajeshwari Pandey, Neeta Pandey, Sajal K. Paul, Mandeep Singh, Manish Jain, "Voltage Mode Biquadratic Filter using Single OTRA," IEEE 5th India International Conference on Power Electronics (IICPE'13), pp. 1- 4, 2012.
33. Pandey, R., Pandey, N., Paul, S. K., Singh, A., Sriram, B., & Trivedi, K.," Voltage mode OTRA MOS-C single input multi output biquadratic universal filter", Advances in Electrical and Electronic Engineering (Theoretical and Applied Electrical Engineering), 10(5), 337–344, 2012.
34. Soliman, A. M., & Madian, A. H., " MOS-C KHN filter using voltage Op-Amp, CFOA, OTRA and DCVC", Journal of Circuits, Systems and Computers, 18(4), 733–769, 2009.
35. Kilinc, S., Keskin, A. U., & Cam, U., " Cascadable voltage-mode multifunction biquad employing single OTRA", Frequenz, 61(3–4), 84–86, 2007.
36. Ghosh, M., Paul, S. K., Ranjan, R. K., & Ranjan, A., " Third order universal filter using single operational transresistance amplifier", Journal of Engineering, Hindawi Publishing Corporation, 2013, Article ID 317296, 1–6, 2013.
37. H. Mostafa, A. M. Soliman, "A modified realization of the operational transresistance amplifier(OTRA)," Frequenz, vol. 60, pp. 70–76, 2006.
38. Prof. Ali M. Niknejad, "Sinusoidal Oscillators: Feedback Analysis", Integrated circuits for communication.
39. Colin Simpson, "Principle of Electronics", 2002, "Chapter 14: Sinusoidal Oscillators".
40. Hung-Chun Chien "Third-Order Sinusoidal Oscillator Using a Single CMOS Operational Transresistance Amplifier" Journal of Applied Science and Engineering, Vol. 19, No. 2, pp. 187196 (2016)
41. Ghanshyam Singh, Md.Hameed Pasha, M.Shashidhar, Zulekha Tabassum, "CMOS realization of OTRA based Electronically Controllable Square Wave Generator Enhancing Linearity with minimum Total Harmonic Distortion and Power Consumption," International Journal of Latest Engineering Science, E-ISSN: 2581-6659, Volume: 02 Issue: 01, January to February 2019.
42. Rajeshwari Pandey, Neeta Pandey, B. Sriram and Sajal K. Paul, "Single OTRA based Multiplier and Its Applications", International Scholarly Research Network ISRN Electronics Volume 2012, Article ID 890615, 7 pages.

43. Vinoth Thyagarajan, Mathivanan "A New Topology For the Design of 3rd Order V-mode Universal Filter with 1 OTRA Using Alpha-Power Model", International Journal of Advanced Research in Management, Architecture, Technology and Engineering (IJARMATE) Vol. 2, Special Issue 12, April 2016, ISSN (ONLINE): 2454-9762
44. John G. Proakis, Masoud Salehi, "Communication Systems Engineering", 2nd Edition, Prentice Hall, New Jersy, "Chapter 7: Digital Transmission Through The Additive White Gaussian Noise Channel", page no.: 345-349
45. B.P. Lathi, Zhi Ding, "Modern Digital And Analog Communication Systems", International Fourth Edition, Oxford University press, "Chapter 1: Introduction", page no.: 1-13.
46. B.P. Lathi, Zhi Ding, "Modern Digital And Analog Communication Systems", International Fourth Edition, Oxford University press, "Chapter4: Amplitude Modulations And Demodulations", page no.: 140-170.
47. Rubi Dhankhar, Sanjeev Pandey, Rajesh Yadav, "Pulse Amplitude Modulation", JIRT, 2015 Volume 1 Issue 12 | ISSN: 2349-6002.